X-rays by Compton Scattering and Sources Driven by SRF Linacs

Geoffrey Krafft, Kirsten Deitrick, Jean Delayen, Randika Gamaga, Todd Satogata

Center for Accelerator Science
Old Dominion University
and
Jefferson Lab

Outline

- Basic Physics
  - Wigglers, Undulators, and Insertion Devices
  - Compton Effect
  - Important Parameters
  - Line Broadening and Narrowing by Chirping
- Laser Performance
  - Self-Excited Arrangements
  - External High Power Optical Cavities
- SRF Compton Sources
  - New Ideas
  - Layout
  - Results

Argonne Advanced Photon Source

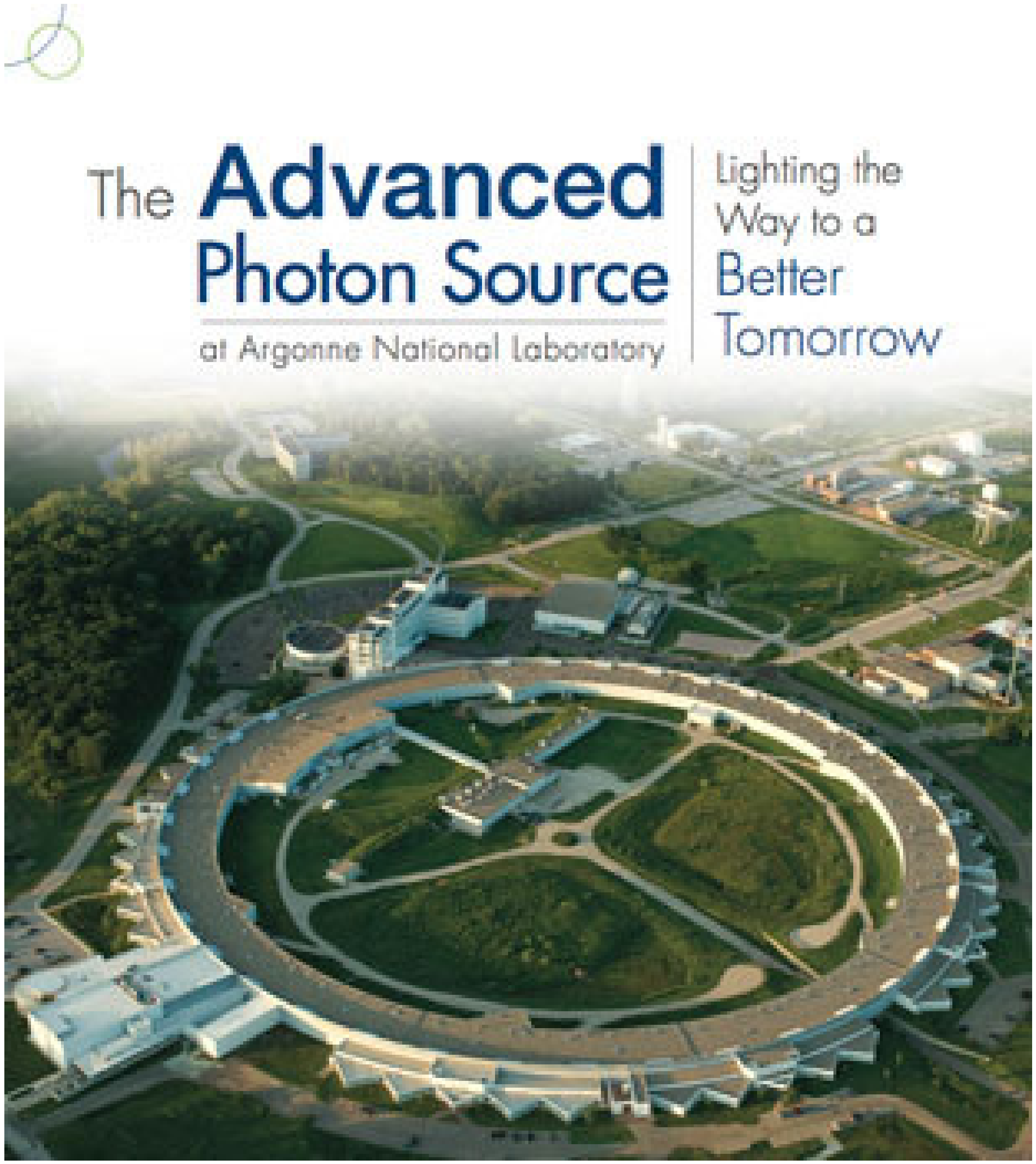

Bend Undulator Wiggler

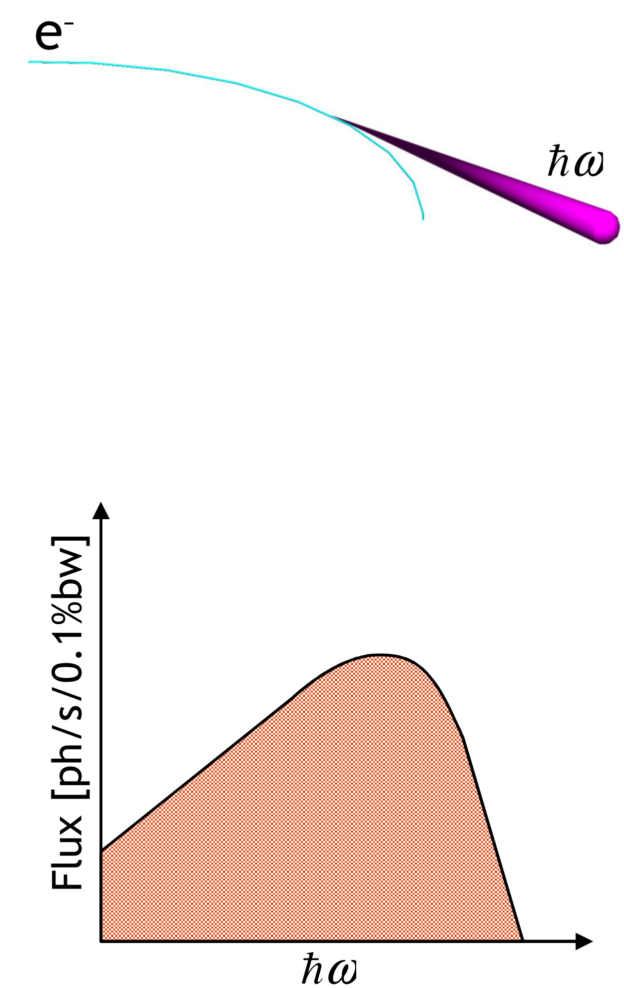

white source

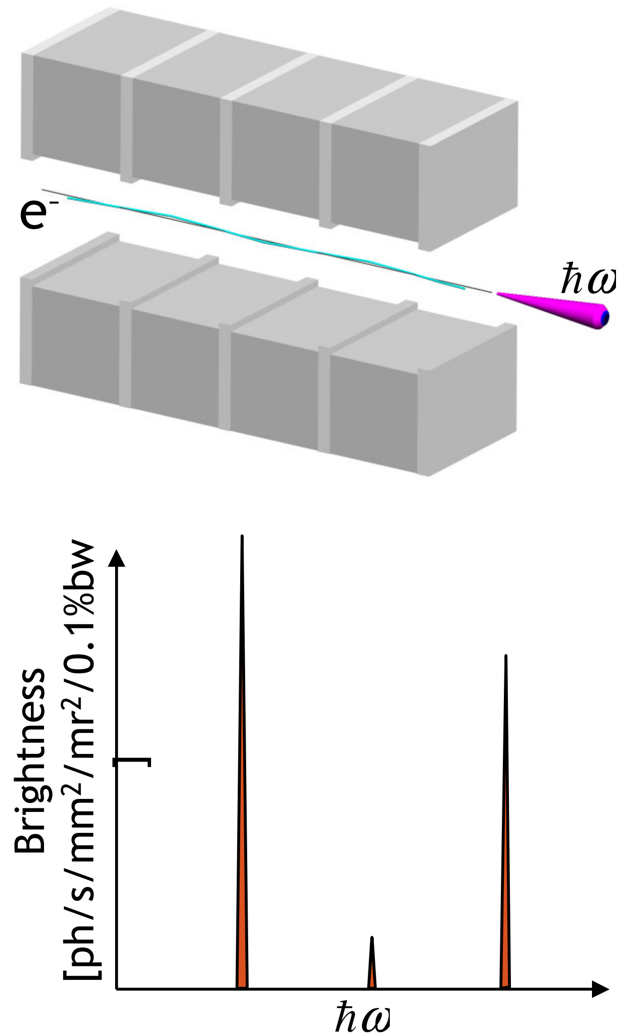

partially coherent source

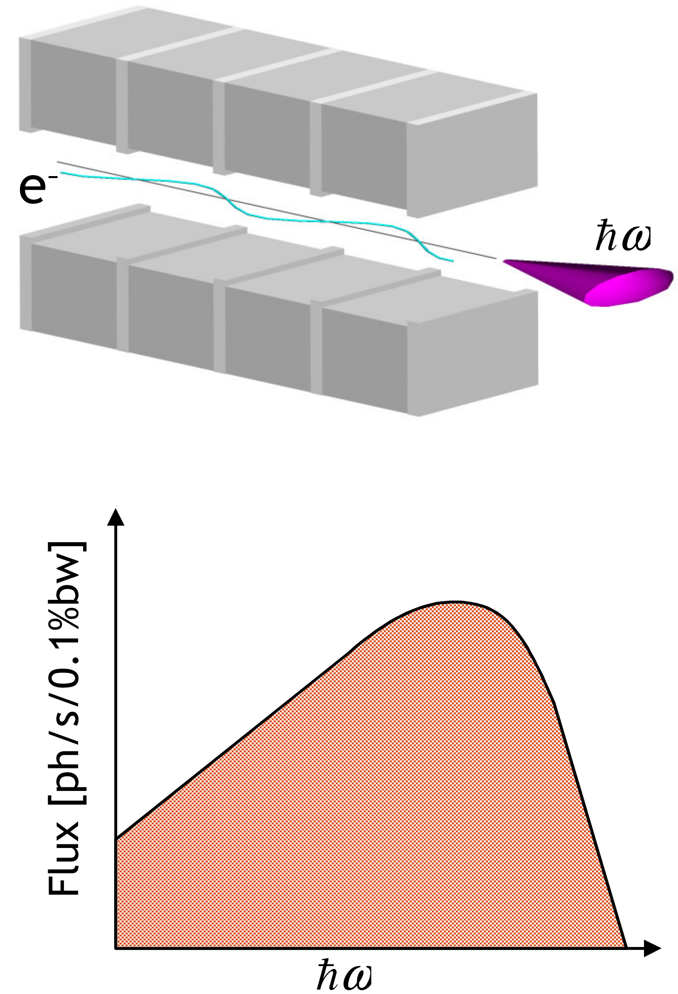

powerful white source

Compton Effect

TABLE I

Wave-length of Primary and Scattered γ-rays

	Angle	μ/ρ	τ/ρ	λ obs.	λ calc.
Primary	0°	.076	.017	0.022 A	(0.022 A)
Scattered	45°	.10	.042	.030	0.029
"	90°	.21	.123	.043	0.047
"	135°	.59	.502	.068	0.063

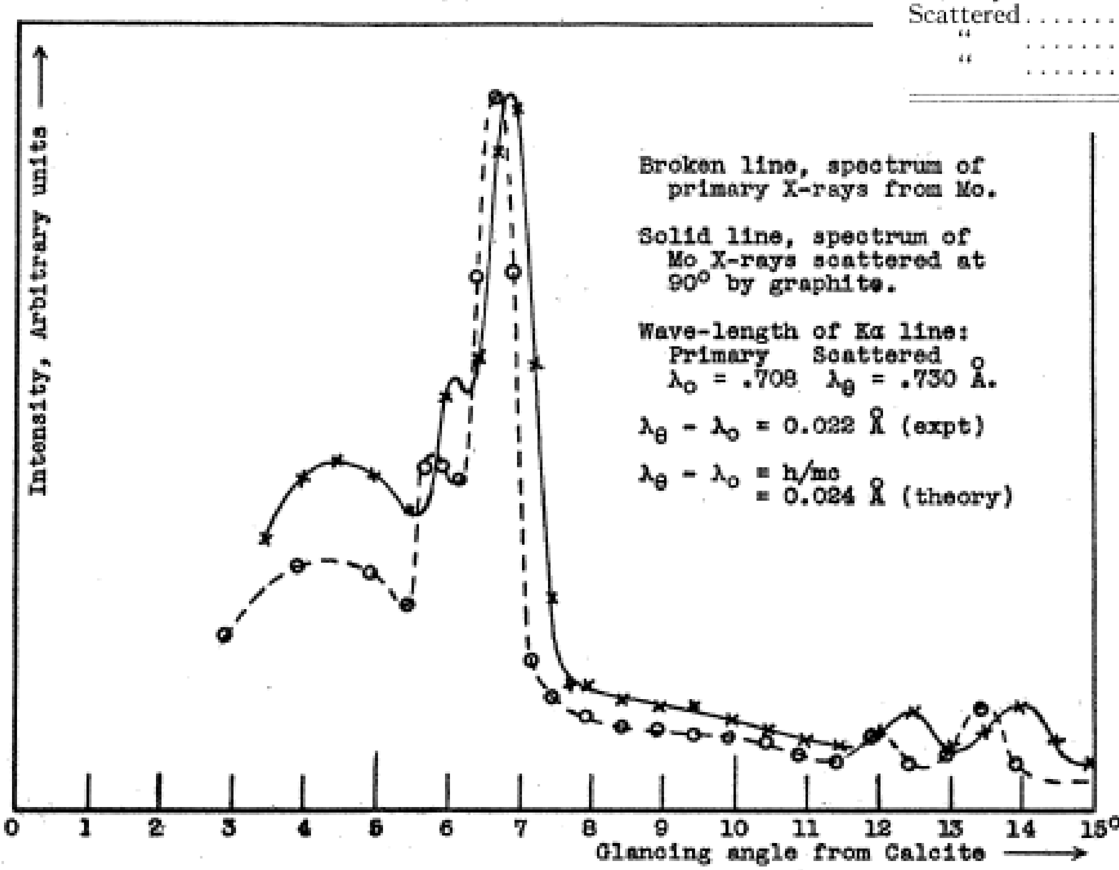

Fig. 4. Spectrum of molybdenum X-rays scattered by graphite, compared with the spectrum of the primary X-rays, showing an increase in wave-length on scattering.

A. H. Compton, Phys. Rev., 21, 483 (1923)

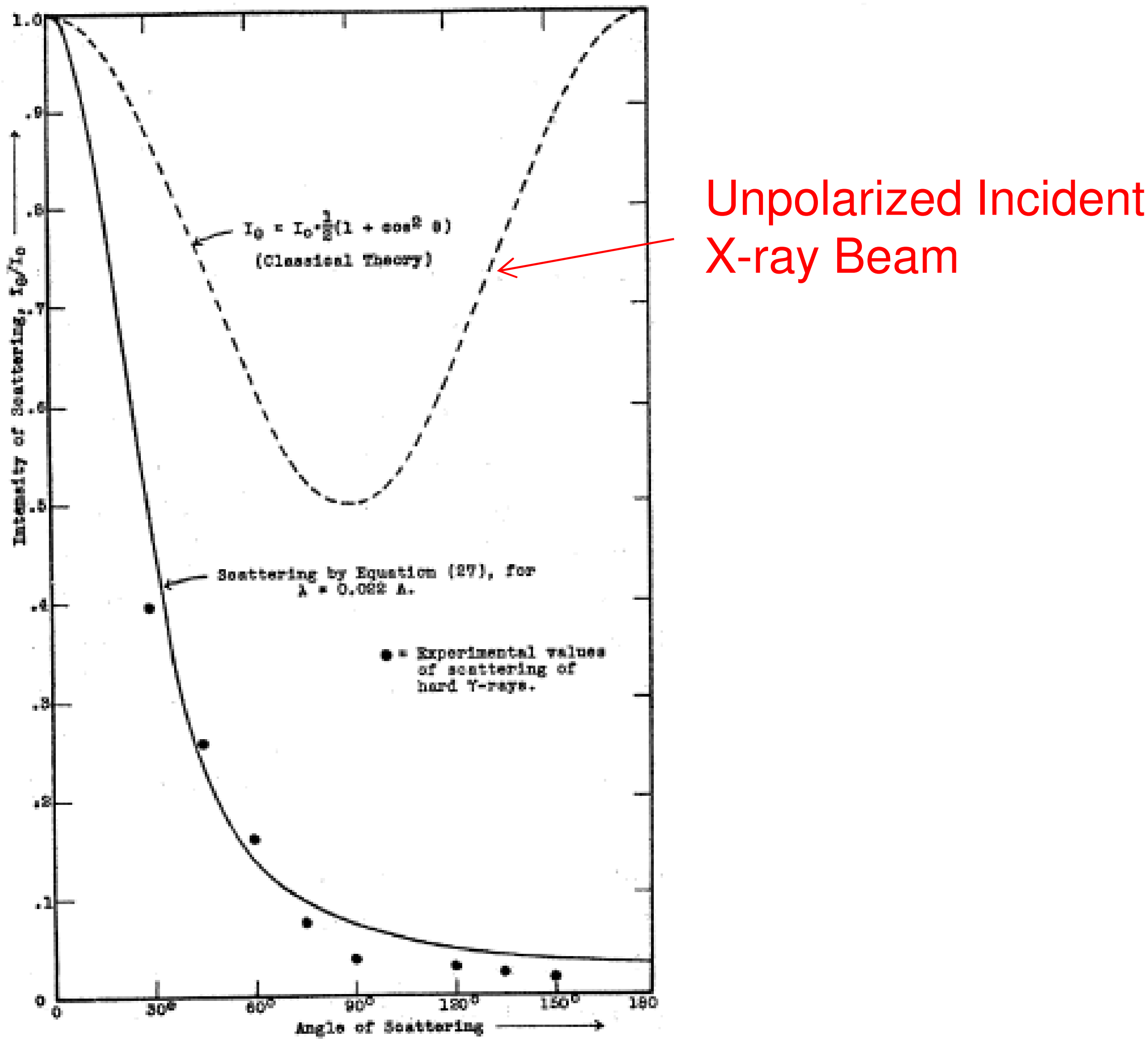

Fig. 7. Comparison of experimental and theoretical intensities of scattered γ-rays.

Scattered Photon Energy

- Layout

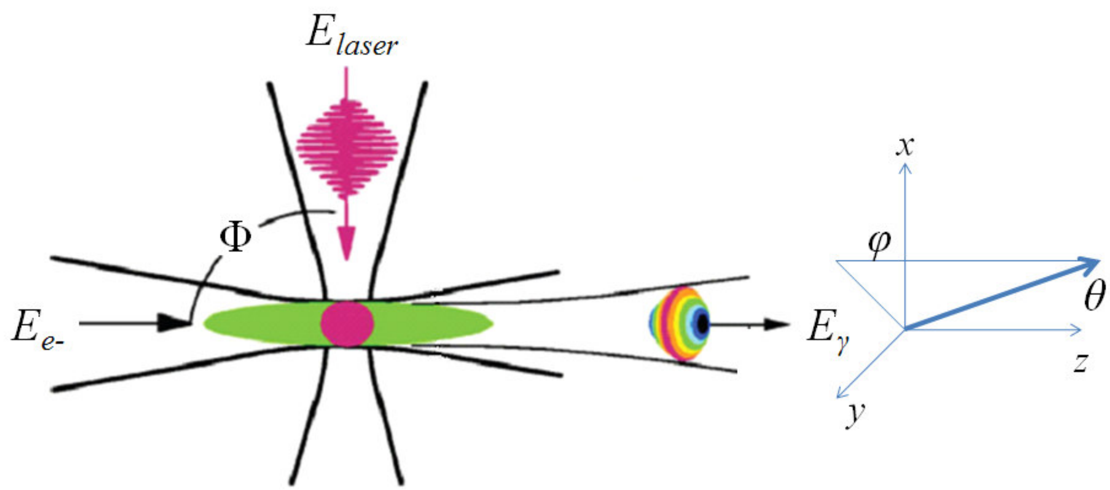

- Energy

$$E_{\gamma}(\theta,\varphi)=\frac{E_{\text{laser}}\left(1-\beta\cos\Phi\right)}{1-\beta\cos\theta+E_{\text{laser}}\left(1-\cos\Delta\Theta\right)/E_{e^-}}$$

- Thomson limit

$$E'_{\text{laser}} << mc^2, \qquad E_{\gamma}\left(\theta,\phi\right)\approx E_{\text{laser}}\frac{1-\beta\cos\Phi}{1-\beta\cos\theta}$$

Field Strength Parameter

- Early 1960s: Laser Invented
- Brown and Kibble (1964): Earliest definition of the field strength parameters (normalized vector potential) *K* and/or *a* in the literature that I'm aware of

$$a = \frac{eE_0\lambda_0}{2\pi mc^2} \quad \text{Compton/Thomson Sources} \qquad K = \frac{eB_0\lambda_0}{2\pi mc} \quad \text{Undulators}$$

  Interpreted frequency shifts that occur at high fields as a "relativistic mass shift".
- Sarachik and Schappert (1970): Power into harmonics at high *K* and/or *a*. Full calculation for CW (monochromatic) laser. Later referenced, corrected, and extended by workers in fusion plasma diagnostics.
- Alferov, Bashmakov, and Bessonov (1974): Undulator/Insertion Device theories developed under the assumption of constant field strength. Numerical codes developed to calculate "real" fields in undulators.
- Coisson (1979): Simplified undulator theory, which works at low *K* and/or *a*, developed to understand the frequency distribution of "edge" emission, or emission from "short" magnets, i.e., including pulse effects

Emission From a "Short" Magnet

Coisson low-field strength undulator spectrum*

$$\frac{dU_\gamma}{d\nu\, d\Omega} = \frac{4 r_e^2 c}{\mu_0} \gamma^2 \left(1+\gamma^2\theta^2\right)^2 f^2 \left|\tilde{B}\left(\nu\left(1+\gamma^2\theta^2\right)/2\gamma^2\right)\right|^2$$

$$f^2 = f_\sigma^2 + f_\pi^2$$

$$f_\sigma = \frac{1}{\left(1+\gamma^2\theta^2\right)^2} \sin\phi$$

$$f_\pi = \frac{1}{\left(1+\gamma^2\theta^2\right)^2} \left(\frac{1-\gamma^2\theta^2}{1+\gamma^2\theta^2}\right) \cos\phi$$

$$r_e^2 \equiv \frac{e^4}{16\pi^2 \varepsilon_0^2 m^2 c^4}$$

*R. Coisson, Phys. Rev. A **20**, 524 (1979)

Dipole Radiation

$$\vec{B} = \frac{\mu_0 e\ddot{d}\left(t - r/c\right)}{4\pi c r}\sin\Theta\hat{\Phi}$$

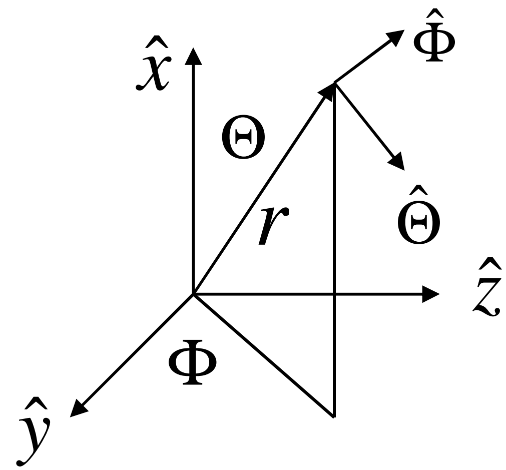

$$\vec{E} = \frac{\mu_0 e\ddot{d}\left(t - r/c\right)}{4\pi r}\sin\Theta\hat{\Theta}$$

$$I = \frac{\vec{E}\times\vec{B}}{\mu_0} = \frac{\mu_0}{16\pi^2}\frac{e^2\ddot{d}^2\left(t - r/c\right)}{c r^2}\sin^2\Theta\hat{r}$$

$$\frac{dP}{d\Omega} = \frac{1}{16\pi^2\varepsilon_0}\frac{e^2\ddot{d}^2\left(t - r/c\right)}{c^3}\sin^2\Theta$$

Polarized in the plane containing $\hat{r} = \vec{n}$ and $\hat{x}$

Define the Fourier Transform

$$\tilde{d}(\omega) = \int d(t) e^{-i\omega t} dt \qquad d(t) = \frac{1}{2\pi} \int \tilde{d}(\omega) e^{i\omega t} d\omega$$

With these conventions Parseval's Theorem is

$$\int d^2(t)\, dt = \frac{1}{2\pi} \int \left|\tilde{d}\right|^2 (\omega)\, d\omega$$

$$\frac{dU_\gamma}{d\Omega} = \frac{e^2}{16\pi^2 \varepsilon_0 c^3} \int \ddot{d}^2 (t - r/c)\ dt = \frac{e^2}{32\pi^3 \varepsilon_0 c^3} \int \omega^4 \left|\tilde{d}\right|^2 (\omega)\ d\omega$$

$$\frac{dU_\gamma}{d\omega d\Omega} = \frac{1}{32\pi^3 \varepsilon_0} \frac{e^2 \omega^4 \left|\tilde{d}(\omega)\right|^2}{c^3} \sin^2 \Theta$$

Blue Sky!

This equation does not follow the typical (see Jackson) convention that combines both positive and negative frequencies together in a single positive frequency integral. The reason is that we would like to apply Parseval's Theorem easily. By symmetry, the difference is a factor of two.

Weak Field Undulator Emission

$$\tilde{\vec{d}}\,'(\omega') = \tilde{d}\,'(\omega')\,\hat{x} = -\frac{ec}{mc}\frac{\tilde{B}\left(\omega'/c\beta_z\gamma\right)}{\omega'^2}\hat{x} \qquad \tilde{B}(k) = \int B(z)e^{-ikz}dz$$

$$\frac{dU_{\gamma,\sigma}}{d\omega d\Omega} = \frac{1}{32\pi^3\varepsilon_0}\frac{e^4}{m^2c^3}\frac{\left|\tilde{B}\left(\omega(1-\beta_z\cos\theta)/c\beta_z\right)\right|^2}{\gamma^2\left(1-\beta_z\cos\theta\right)^2}\sin^2\phi$$

$$\frac{dU_{\gamma,\pi}}{d\omega d\Omega} = \frac{1}{32\pi^3\varepsilon_0}\frac{e^4}{m^2c^3}\frac{\left|\tilde{B}\left(\omega(1-\beta_z\cos\theta)/c\beta_z\right)\right|^2}{\gamma^2\left(1-\beta_z\cos\theta\right)^2}\left(\frac{\cos\theta-\beta_z}{1-\beta_z\cos\theta}\right)^2\cos^2\phi$$

$$\lambda = \frac{\lambda_0}{2\gamma^2} \qquad (1-\beta_z\cos\theta)(1+\beta_z) \approx \frac{1}{\gamma^2}+\theta^2+\ldots \approx \frac{1+\gamma^2\theta^2}{\gamma^2}$$

Generalizes Coisson results to arbitrary observation angles

Weak Field Thomson Backscatter

With $\Phi = \pi$ and $a << 1$ the result is identical to the weak field undulator result with the replacement of the magnetic field Fourier transform by the electric field Fourier transform

	Undulator	Thomson Backscatter
Driving Field	$c\tilde{B}_y\left(\omega(1-\beta_z\cos\theta)/c\beta_z\right)$	$\tilde{E}_x\left(\omega(1-\beta_z\cos\theta)/\left(c(1+\beta_z)\right)\right)$
Forward Frequency	$\lambda \approx \dfrac{\lambda_0}{2\gamma^2}$	$\lambda \approx \dfrac{\lambda_0}{4\gamma^2}$
	Lorentz contract + Doppler	Double Doppler

Handy Formulas

$$\frac{d^2U_\gamma}{d\omega d\Omega} = \frac{r_e^2\varepsilon_0}{2\pi c}\left|\tilde{E}\left[\frac{\omega(1-\beta\cos\theta)}{c(1+\beta)}\right]\right|^2 \times$$

$$\frac{\sin^2\phi(1-\beta\cos\theta)^2 + \cos^2\phi(\cos\theta-\beta)^2}{\gamma^2(1-\beta\cos\theta)^{2\cdot 2}}$$

$$U_\gamma = \gamma^2(1+\beta)\frac{N_e\sigma_T}{(\sigma_e^2+\sigma_{laser}^2)}U_{laser}$$

$$N_\gamma = \sigma_T\frac{N_eN_{laser}}{2\pi(\sigma_e^2+\sigma_{laser}^2)}$$

$$N_{\gamma,\mathrm{per}\ e} = \frac{2\pi\alpha N_\lambda a^2}{3}$$

Number Distribution of Photons

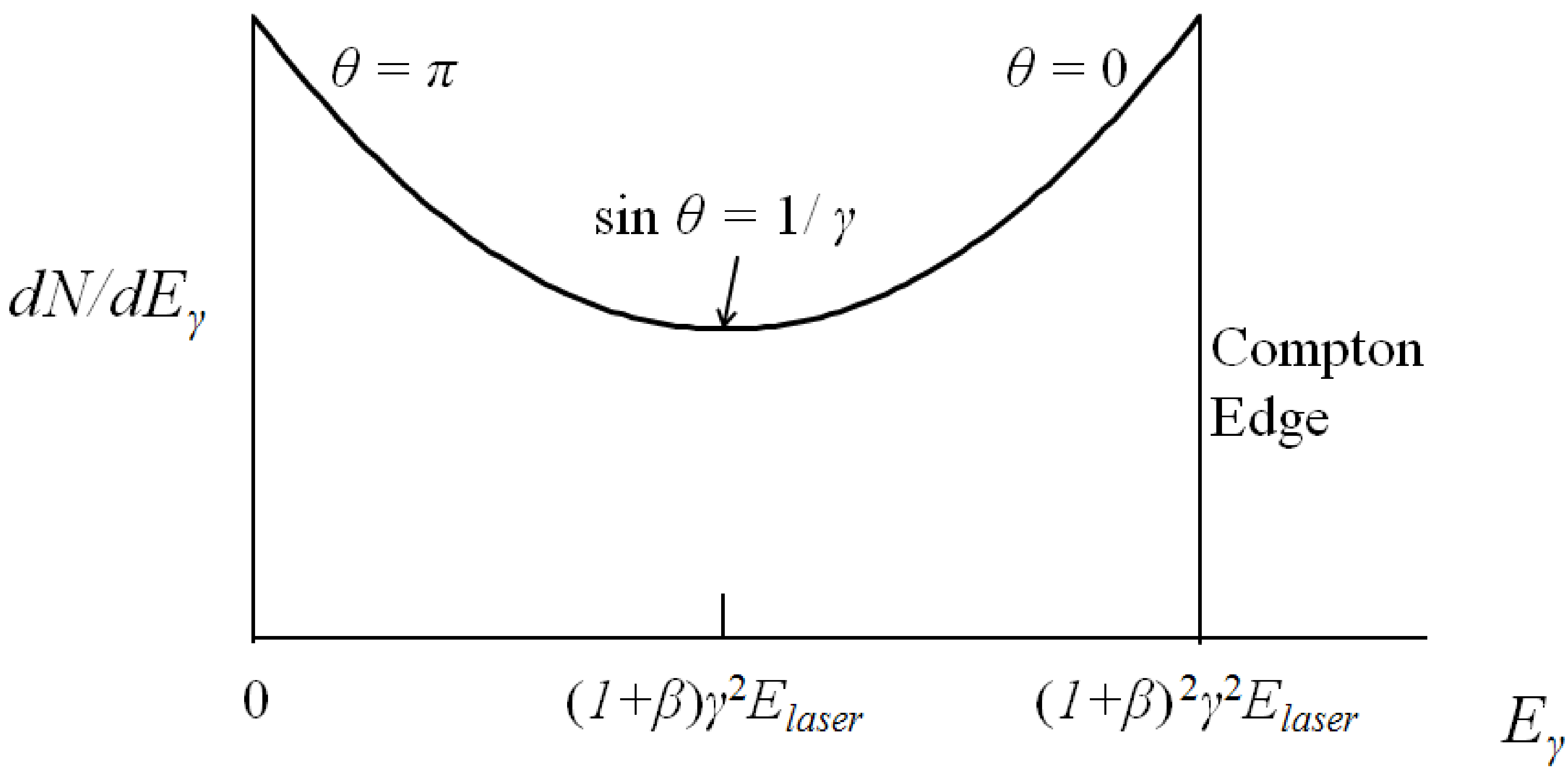

Flux

- Percentage in 0.1% bandwidth ($\theta = 0$)

$$N_{0.1\%} = 1.5\times10^{-3} N_{\gamma}$$

- Flux into 0.1% bandwidth

$$\mathrm{F} = 1.5\times10^{-3} \dot{N}_{\gamma}$$

- Flux for high rep rate source

$$\mathrm{F} = 1.5\times10^{-3} f N_{\gamma}$$

Scattered Photon Energy Spread

Source Term	Estimate	Comment
Beam energy spread	$2\sigma_{E_{e-}} / E_{e-}$	From FEL resonance
Laser pulse width	σ_ω / ω	Doppler Freq Independent
Finite θ acceptance (full width)	$\gamma^2 \Delta\theta^2$	$\theta = 0$ for experiments
Finite beam emittance	$2\gamma^2 \varepsilon / \beta_{e-}$	Beta-function

Spectral Brilliance

- In general

$$B = \frac{F}{4\pi^2 \sigma_x \sigma_{x'} \sigma_y \sigma_{y'}}$$

$$\approx \frac{F}{4\pi^2 \sqrt{\beta_x \varepsilon_x} \sqrt{\varepsilon_x / \beta_x + \lambda / 2L} \sqrt{\beta_y \varepsilon_y} \sqrt{\varepsilon_y / \beta_y + \lambda / 2L}}$$

- For Compton scattering from a low energy beam

$$B = \frac{F}{4\pi^2 \varepsilon_x \varepsilon_y}$$

High *a/K*

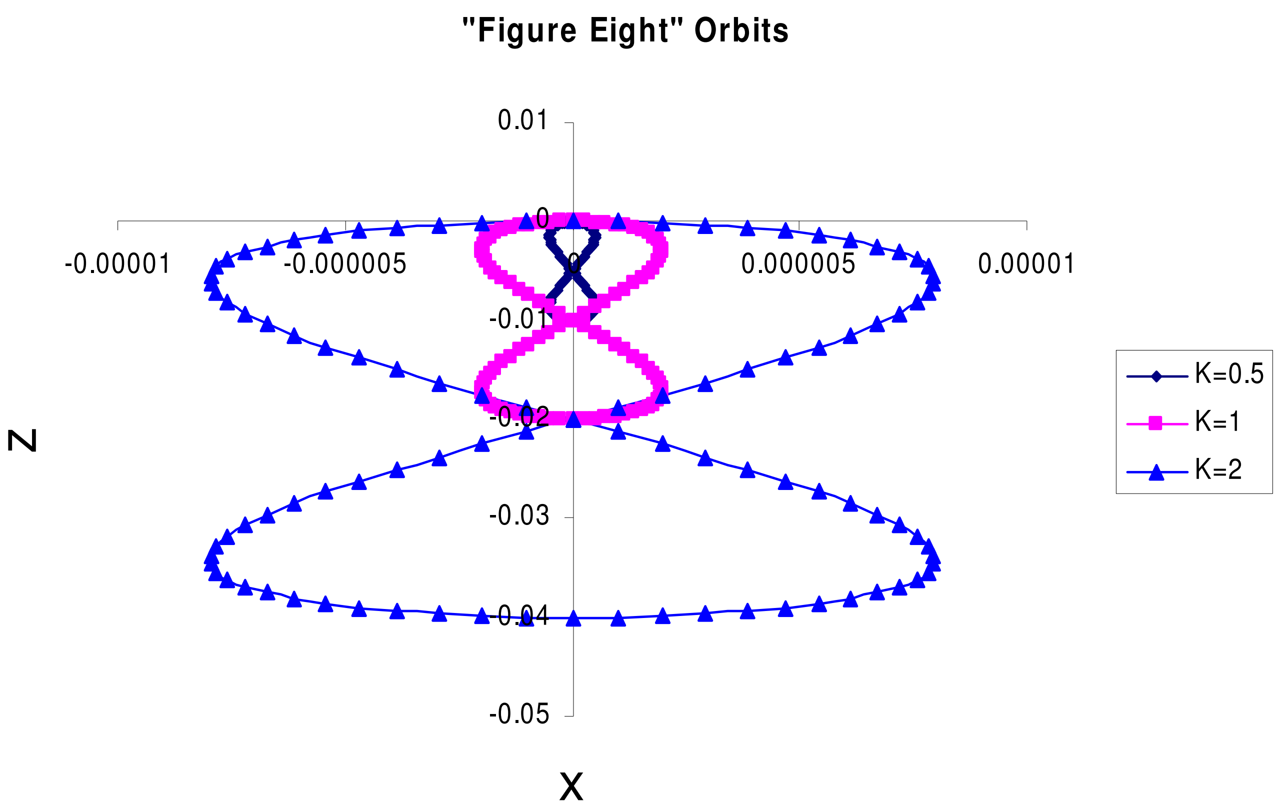

$\gamma = 100$, distances are normalized by $\lambda_0 / 2\pi$

“Effective” Dipoles

$$D_t(\omega;\theta,\varphi)=\frac{1}{\gamma(1-\beta\cos\Phi)}\int\frac{eA(\xi)}{mc}e^{i\phi(\omega,\xi;\theta,\varphi)}d\xi$$

$$D_p(\omega;\theta,\varphi)=\frac{1}{\gamma(1-\beta\cos\Phi)}\int\frac{e^2A^2(\xi)}{2m^2c^2}e^{i\phi(\omega,\xi;\theta,\varphi)}d\xi$$

And the (Lorentz invariant!) phase is

$$\varphi(\omega,\xi;\theta,\phi)=\frac{\omega}{c}\left(\begin{array}{l}\xi\frac{(1-\beta\cos\theta)}{(1-\beta\cos\Phi)}-\frac{\sin\theta\cos\phi}{\gamma(1-\beta\cos\Phi)}\int_{-\infty}^{\xi}\frac{eA(\xi')}{mc}d\xi' \\ +\frac{1-\sin\theta\sin\phi\sin\Phi-\cos\theta\cos\Phi}{\gamma^2(1-\beta\cos\Phi)^2}\int_{-\infty}^{\xi}\frac{e^2A^2(\xi')}{2m^2c^2}d\xi'\end{array}\right)$$

High Field Backscatter

For a flat incident laser pulse the main results are very similar to those from undulaters with the following correspondences

	Undulator	Thomson Backscatter
Field Strength	K	a
Forward Frequency	$\lambda \approx \frac{\lambda_0}{2\gamma^2}\left(1+\frac{K^2}{2}\right)$	$\lambda \approx \frac{\lambda_0}{4\gamma^2}\left(1+\frac{a^2}{2}\right)$
Transverse Pattern	$\beta^*_z + \cos\theta'$	$1+\cos\theta'$

NB, be careful with the radiation pattern, it is the same at small angles, but quite a bit different at large angles

Ponderomotive Broadening

$$A_x(\xi) = A_{peak}\exp\left(-z^2/2(8.156\lambda_0)^2\right)\cos\left(2\pi\xi/\lambda_0\right) \qquad a_{peak} = eA_{peak}/mc$$

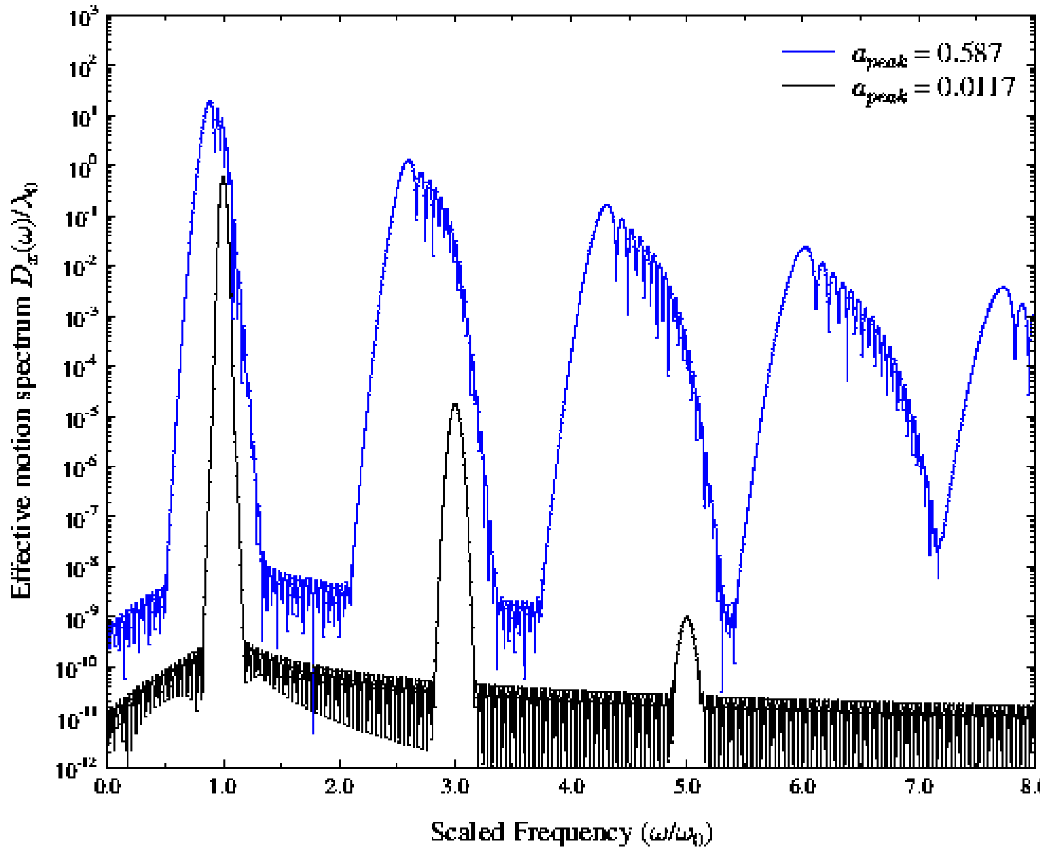

G. A. Krafft, Phys. Rev. Lett., **92**, 204802 (2004)

Compensation By “Chirping”

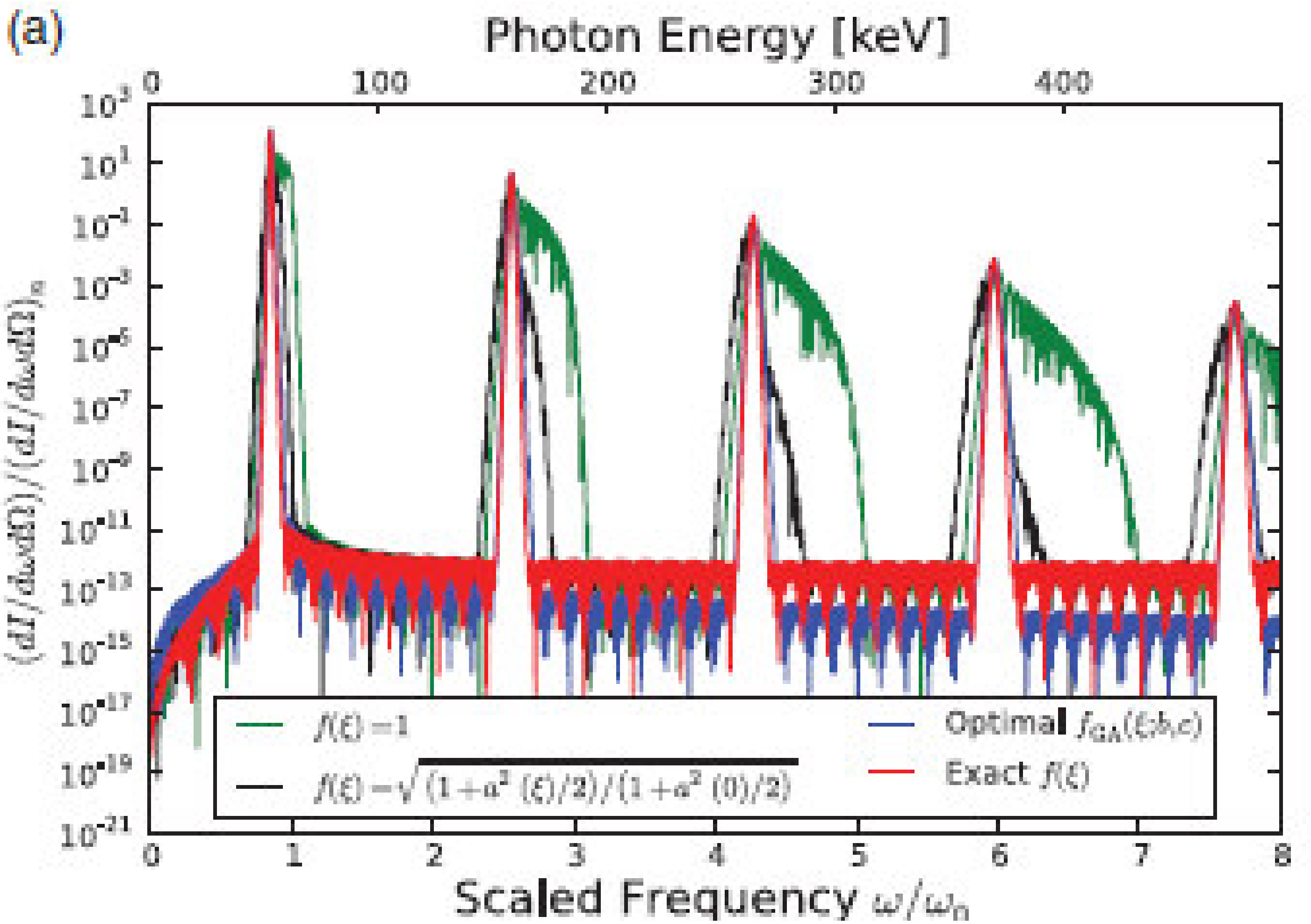

Terzic, Deitrick, Hofler, and Krafft,
Phys. Rev. Lett., **112**, 074801 (2014)

$$f(\xi) = \frac{1}{1+a^2(0)/2}\left(1 + \frac{\int_0^\xi a^2(\xi')d\xi'}{2\xi}\right)$$

Beam Illumination Methods

- Direct illumination by laser
  - Earliest method
  - Deployed on storage rings

- Optical cavities
  - Self-excited
  - Externally excited
  - Deployed on rings, linacs, and energy recovered linacs

Early Gamma Ray Source

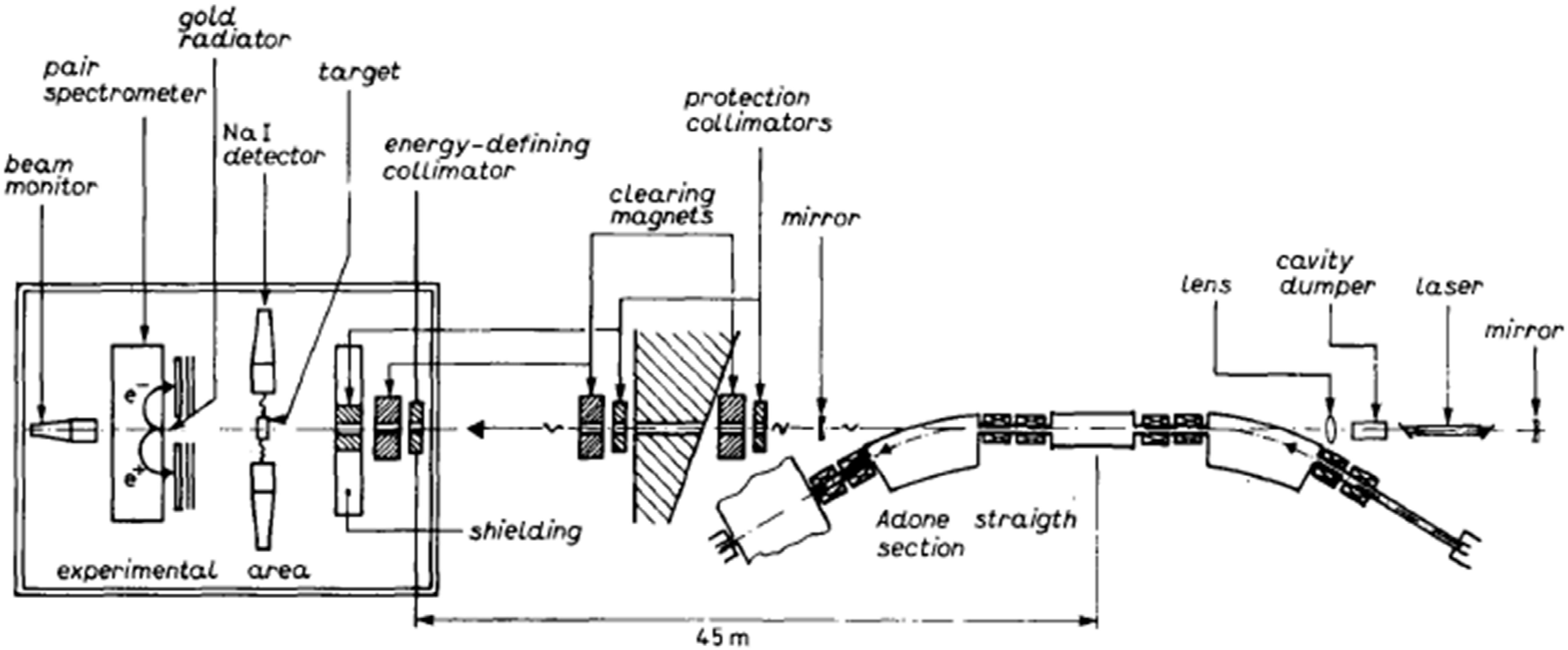

Fig. 1. – Overall view of the experimental set-up.

Compton Edge
78 MeV

Federici, *et al.*
Nouvo. Cim. B 59, 247 (1980)

Optical Cavities

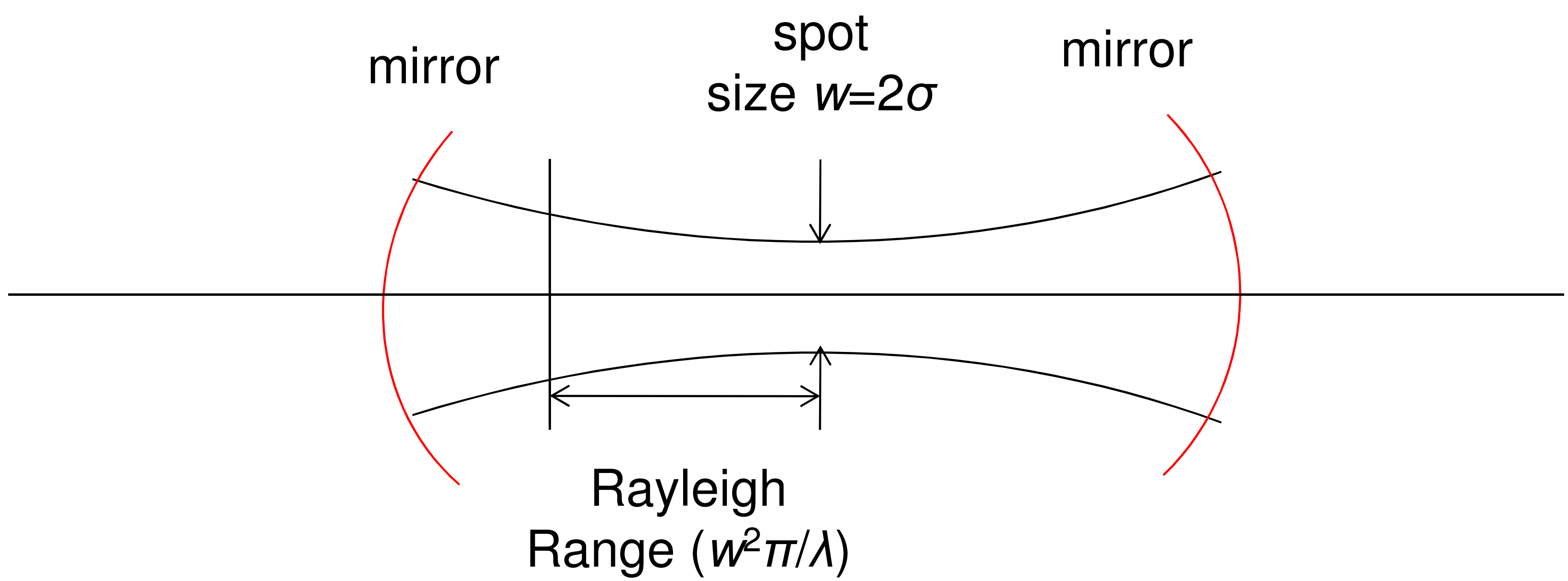

Quantity	Dimensions
Wavelength	200 nm-10 microns
Circulating Power	0.1-200 kW
Spot Size	50-500 microns
Rayleigh Range	40 cm-5 m

Self Excited

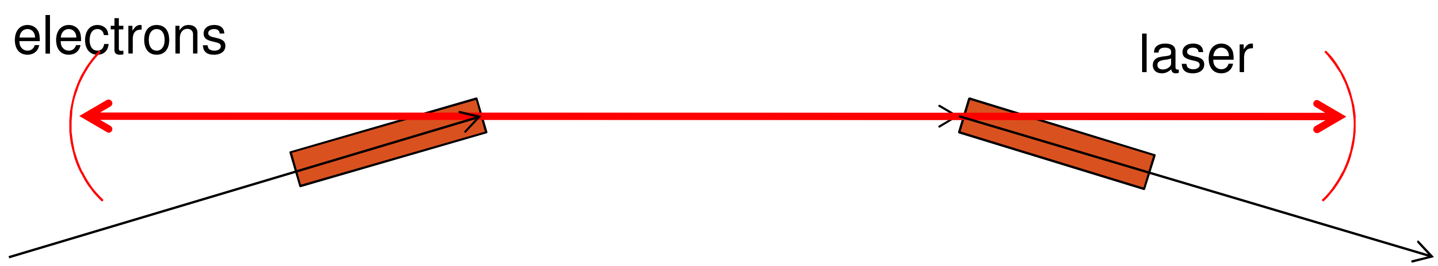

Location	Wavelength	Circulating Power	Spot Size	Rayleigh Range
Orsay	5 microns	100 W	mm	0.7 m
UVSOR	466 nm	20 W	250 microns	0.4 m
Duke Univ.	545 nm	1.6 kW	930 microns	5 m
Super-ACO	300 nm	190 W	440 microns	2 m
Jefferson Lab FEL	1 micron	100 kW	150 microns	1 m

Externally Excited

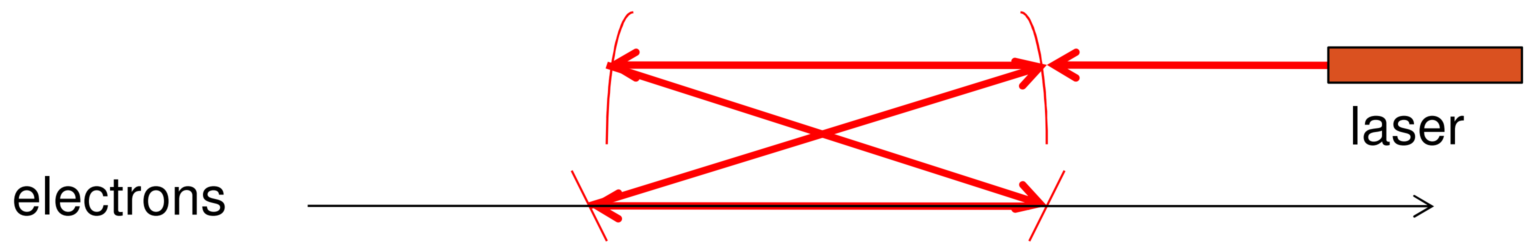

Location	Wavelength	Input Power	Circulating Power	Spot Size (rms)
Jefferson Lab Polarimeter	1064 nm	0.3 W	1.5 kW	120 microns
TERAS	1064 nm	0.5 W	7.5 W	900 microns
Lyncean	1064 nm	7 W	25 kW	60 microns
HERA Polarimeter	1064 nm	0.7 W	2 kW	200 microns
LAL	532 nm	1.0 W	10 kW	40 microns

Lyncean Compact X-ray Source

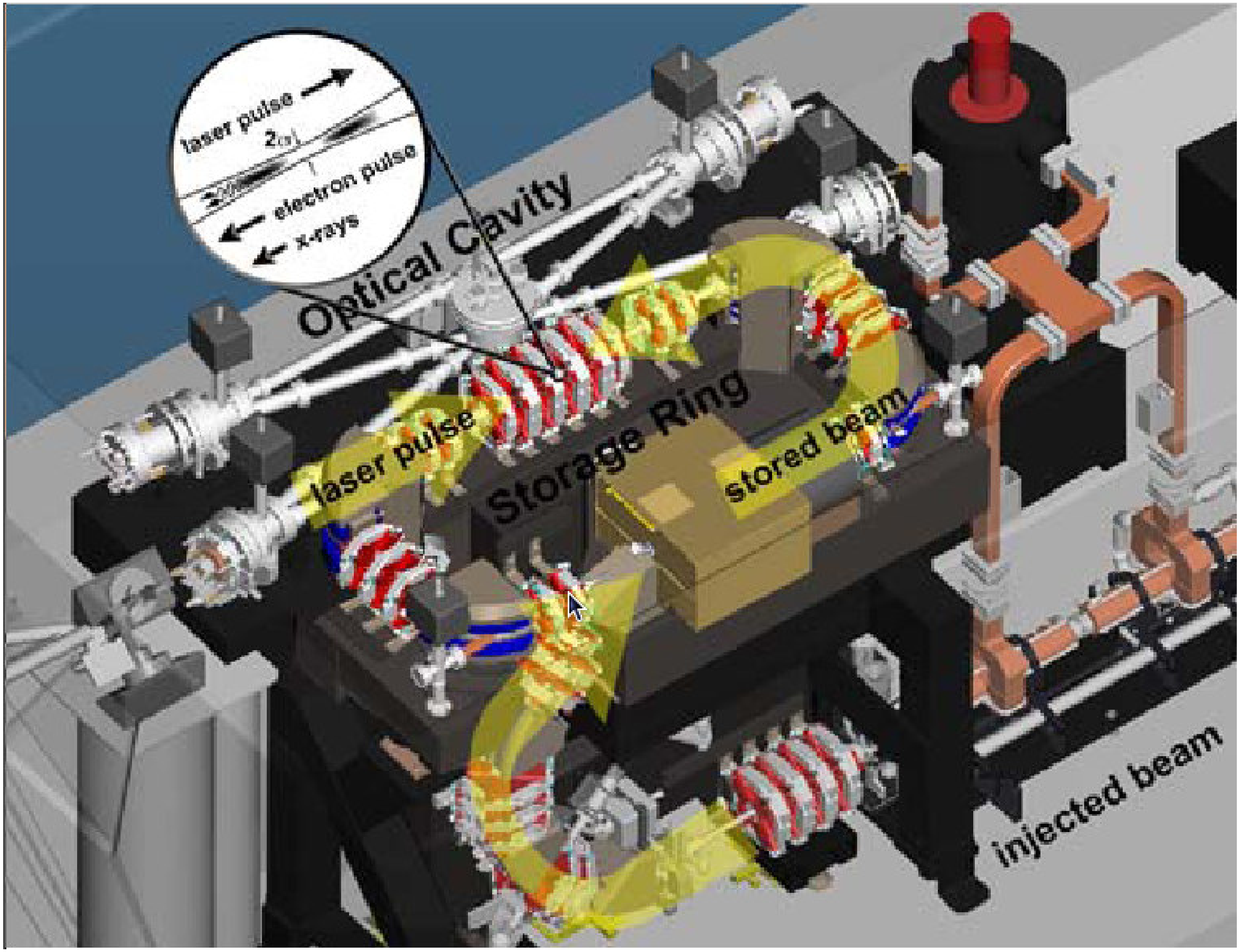

Lyncean Source Performance

Parmeter	Value	Unit
Photon Energy	10-20	keV
Production Rate	10^{11}	photons/sec
Laser Wavelength	1064	nm
Circulating Power	25	kW
Polarization	100%	
Ultimate Brilliance	5×10^{11}	p/(sec mm^{2}mrad^{2}0.1%)

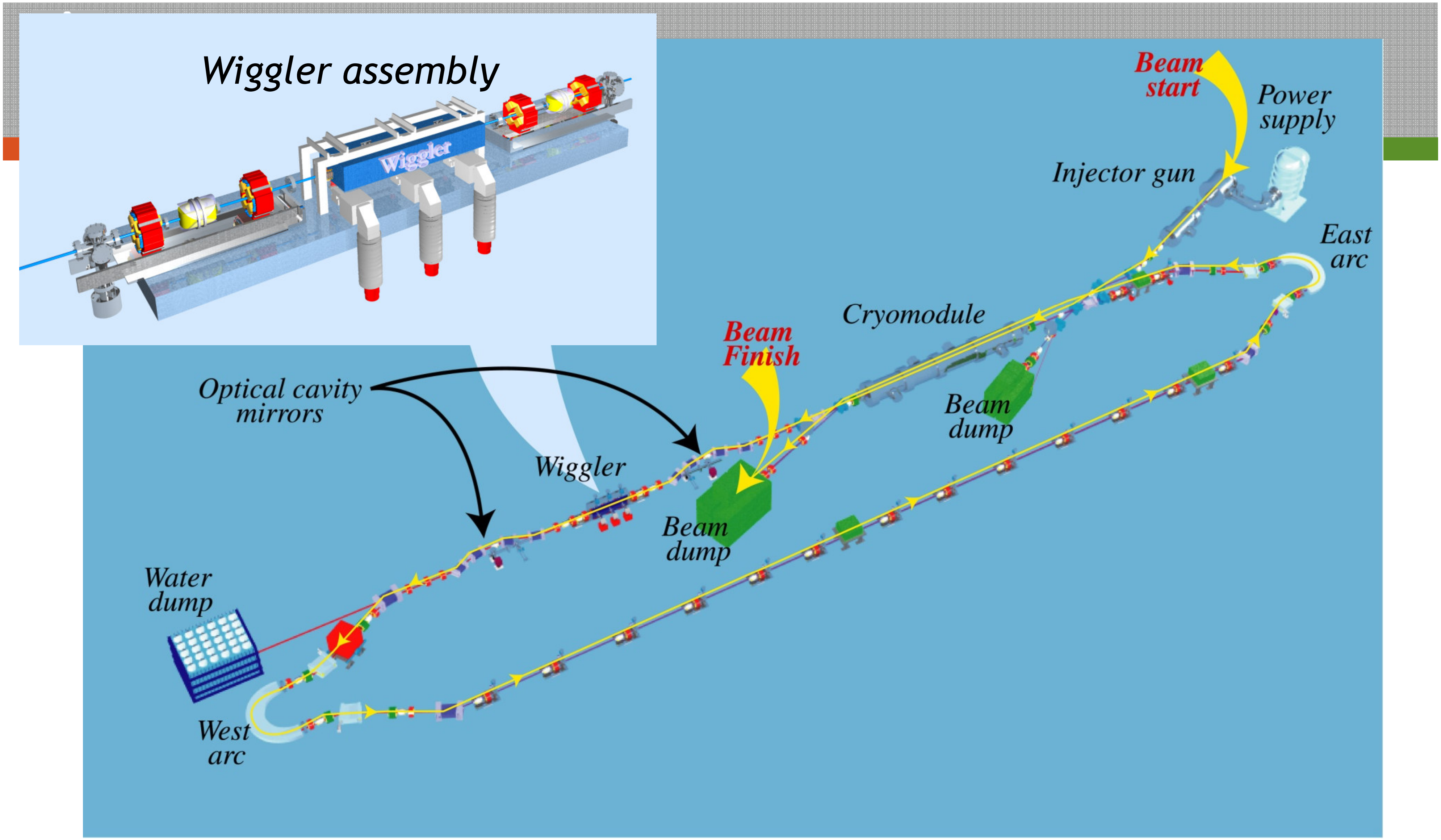

Neil, G. R., *et. al, Physical Review Letters,* **84,** 622 (2000)

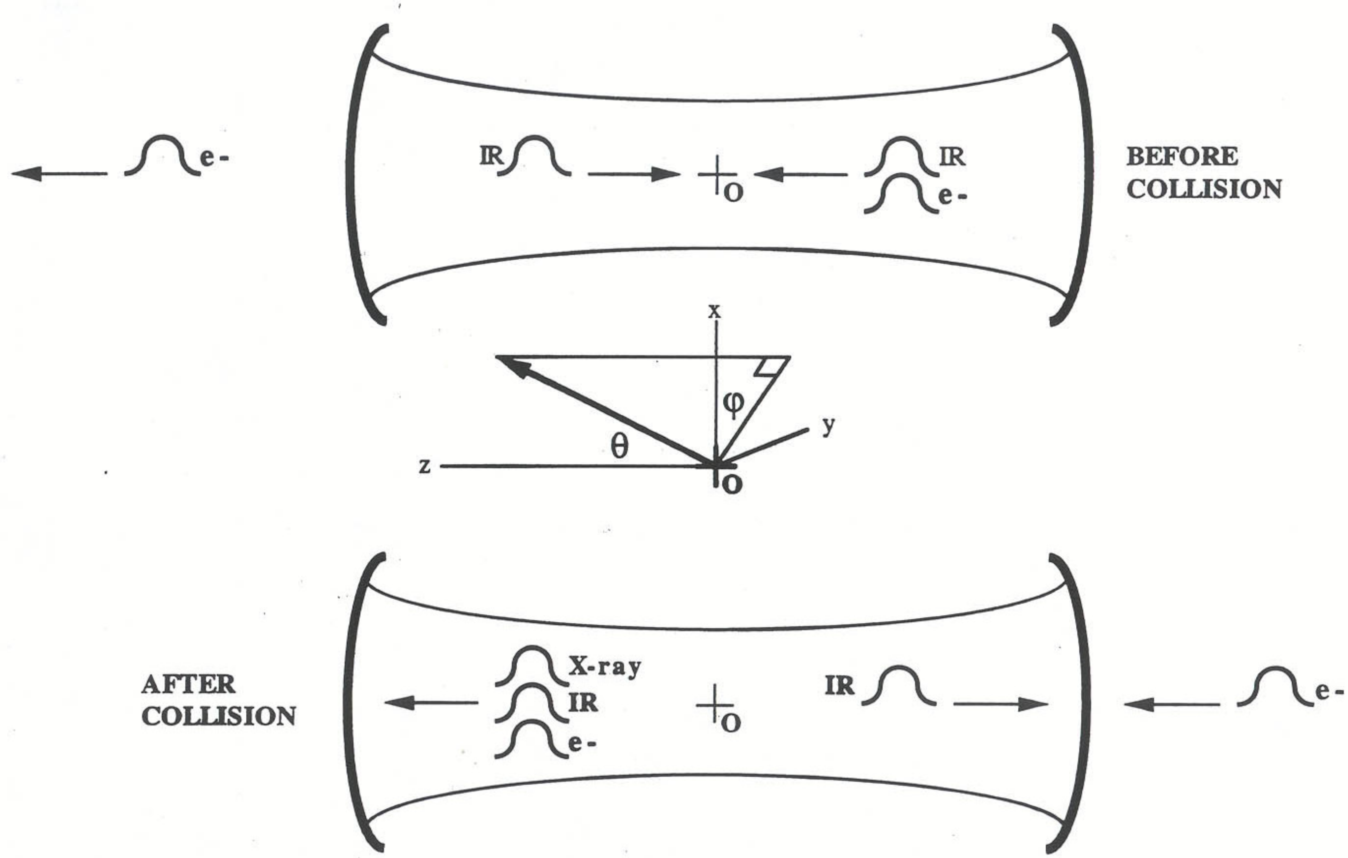

SCATTERING GEOMETRY

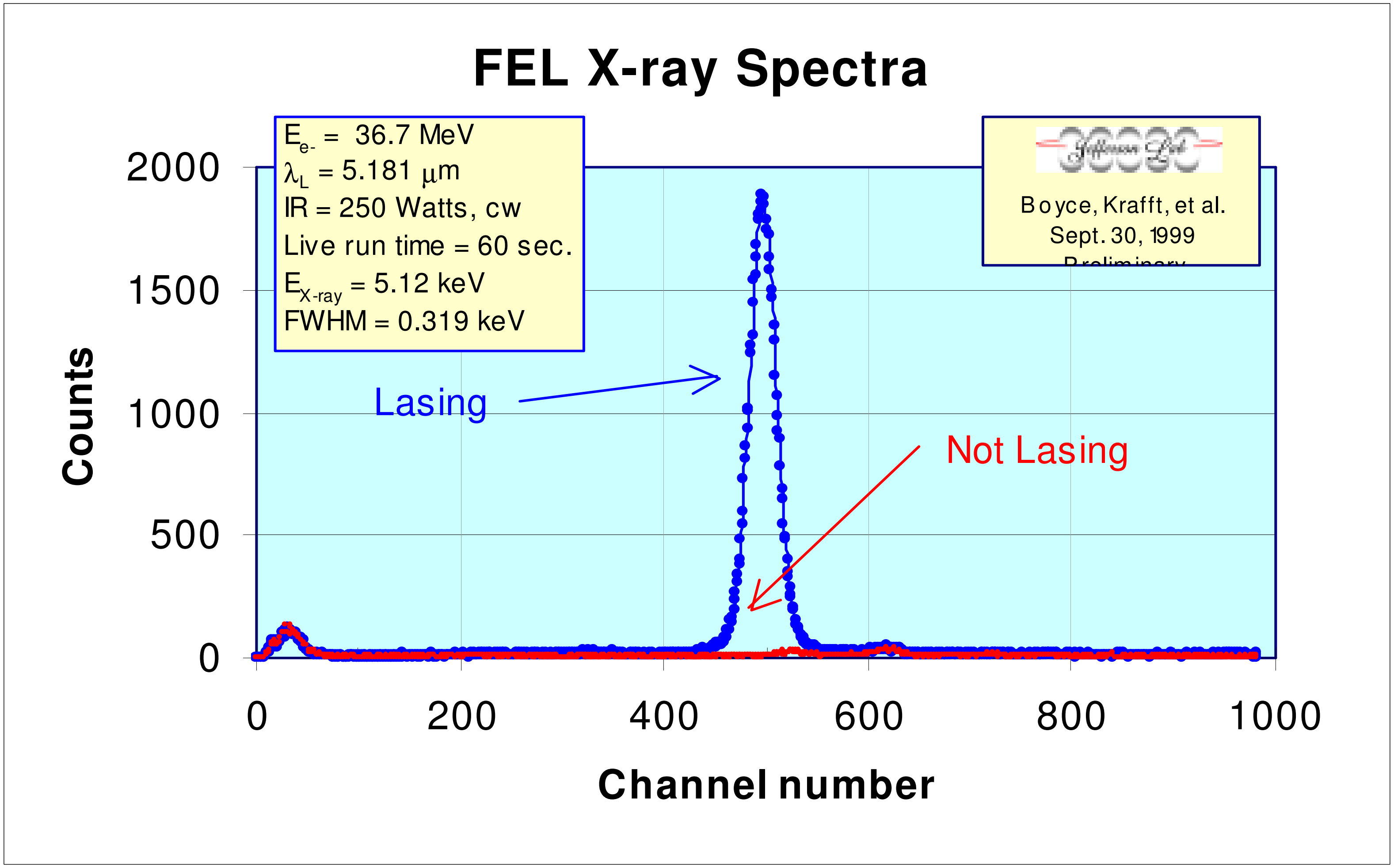

Boyce, *et al.*, 17th Int. Conf. Appl. Accel., 325 (2002)

High Power Optical Cavities

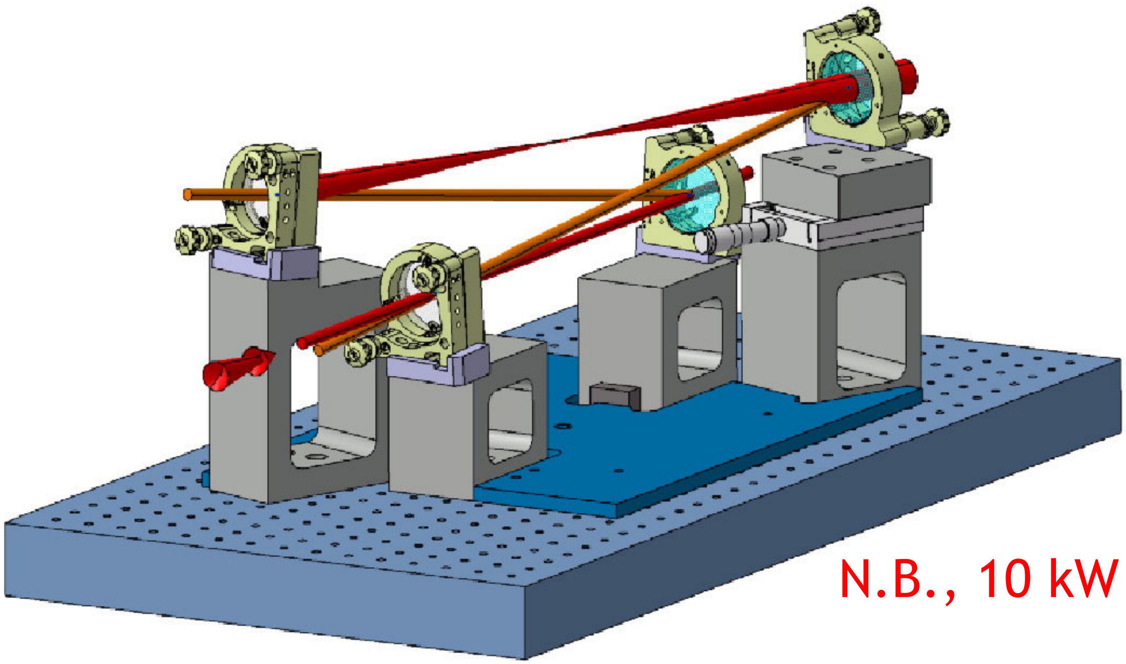

V. Brisson, *et al.*, *NIM A*, **608**, S75 (2009)

N.B., 10 kW FEL there, sans spot!

In this paper we described our first results on the locking of a Ti:sapph oscillator to a high finesse FPC. For the first time, to our knowledge, we demonstrate the possibility of stacking picosecond pulses inside an FPC at a very high repetition rate with a gain of the level of 10000. By studying the stability of four-mirrors resonators, we developed a new promising nonplanar geometry that we have just started to study experimentally. Finally, we mentioned that we shall next use the recent and powerful laser fiber amplification scheme to reach the megawatt average power inside FPC as required by the applications of the Compton X and gamma ray sources.

LAL/Thales THomX

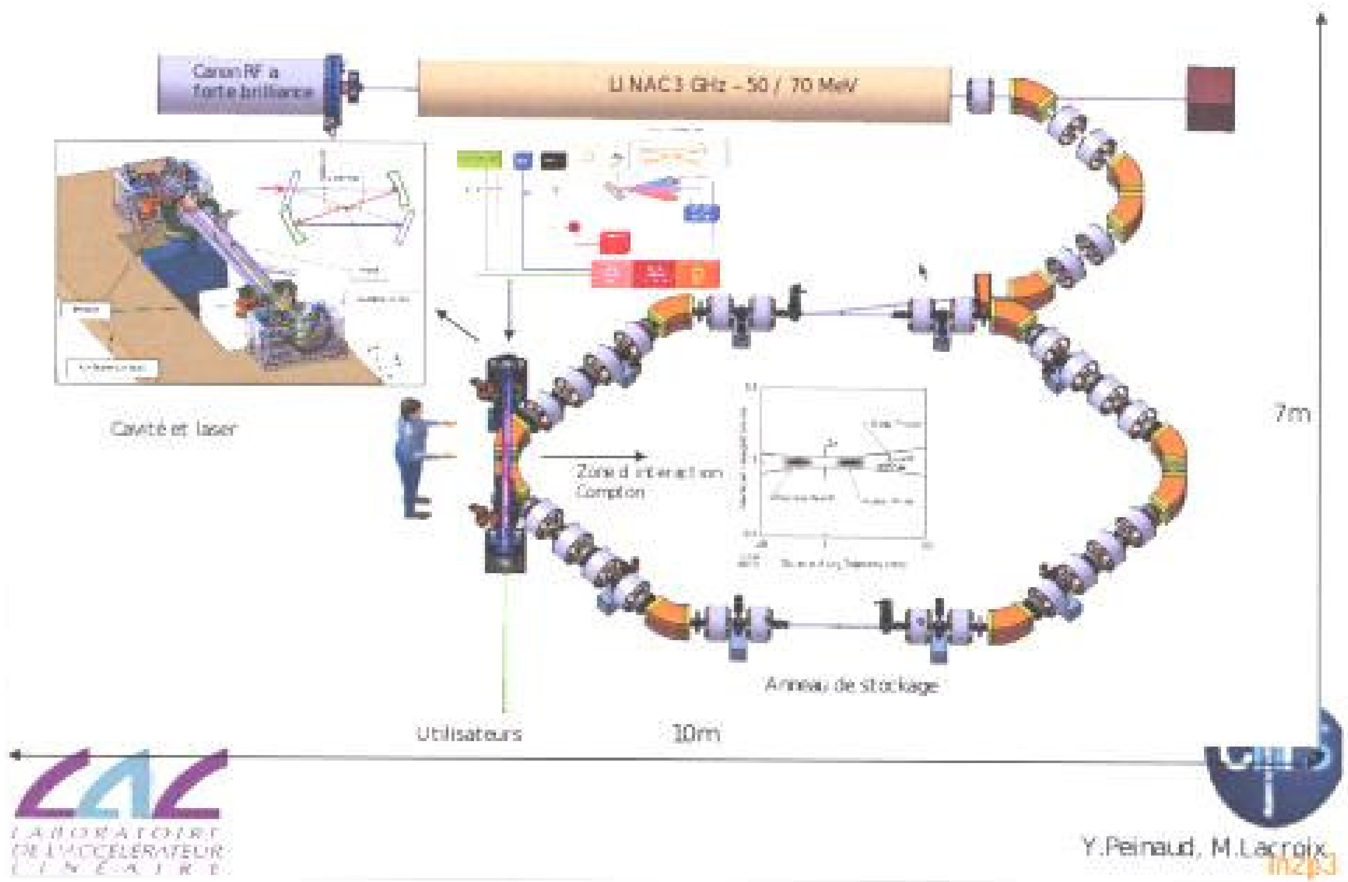

BES Workshop on Compact Light Sources (2010)

Hajima, et al.

Uranium Detection

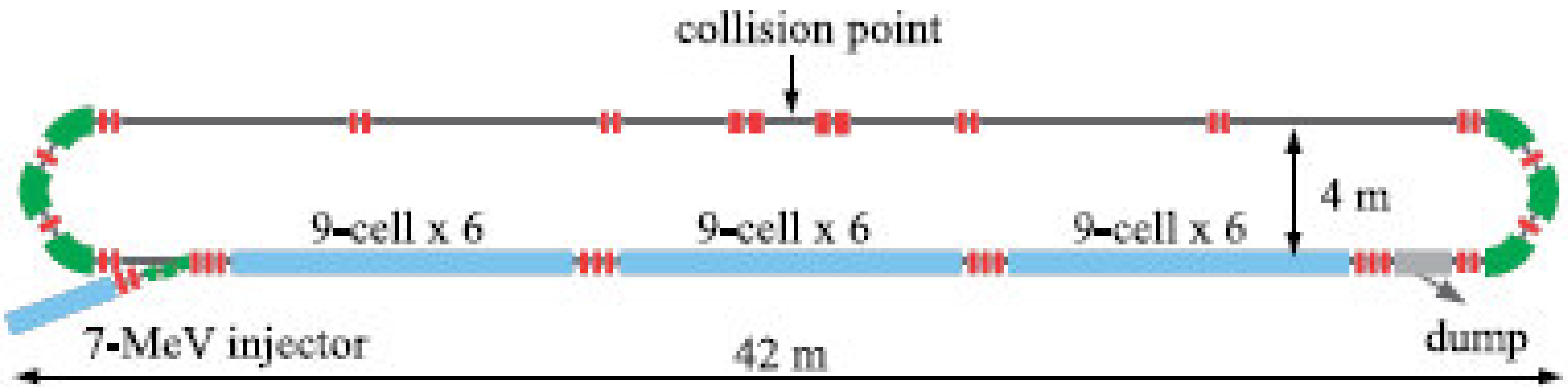

Fig. 3. Layout of the 350-MeV ERL designed for a high-flux γ-ray source. An electron beam generated by the 7-MeV injector is accelerated up to 350 MeV by the main linac and transported to the recirculation loop. The collision point for LCS γ-ray generation is located in the middle of the straight section.

Hajima, *et al., NIM A*, **608**, S57 (2009)
TRIUMF Moly Source?

MIT CUBiX

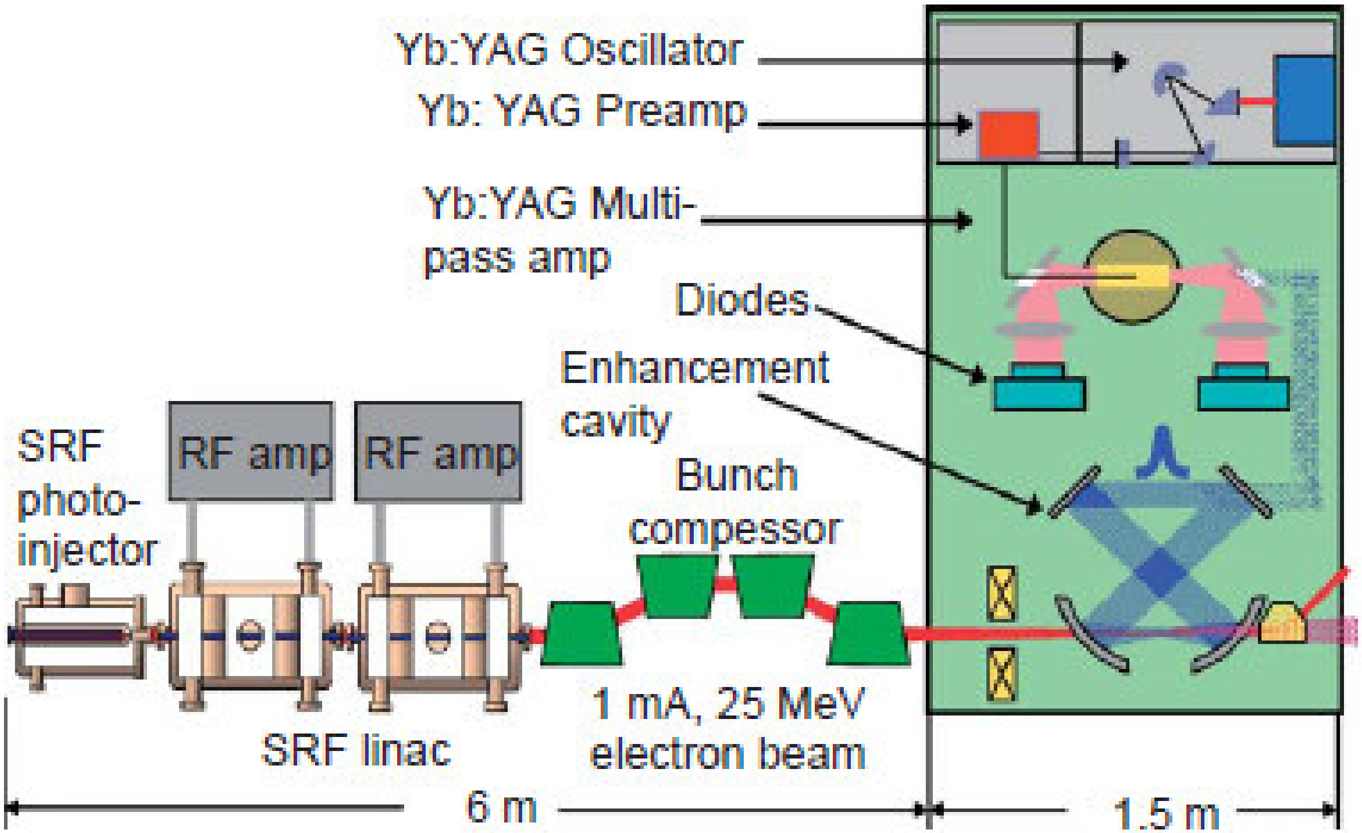

Fig. 2. Major technical components including cryocooled high-power laser and SRF linac.

Graves, *et al., NIM A*, **608**, S103 (2009)

Table 1
X-ray parameters.

Parameter	Single shot	High flux
Tunable photon energy (keV)	3–30	
Pulse length (ps)	2	0.1
Flux per shot (photons)	1×10^{10}	3×10^{6}
Repetition rate (Hz)	10	10^{8}
Average flux (photons/s)	1×10^{11}	3×10^{14}
On-axis bandwidth (%)	2	1
RMS divergence (mrad)	5	1
Source RMS size (mm)	0.006	0.002
Peak brilliance (photons/(s mm^2 mrad^2 0.1%bw))	6×10^{22}	6×10^{19}
Average brilliance (photons/(s mm^2 mrad^2 0.1%bw))	6×10^{11}	2×10^{15}

numerical simulation results assuming parameters of $E = 25\,\text{MeV}$, $\varepsilon_{nx} = 0.1\ \mu\text{m}$, $x_e = 2\ \mu\text{m}$, $\Delta t_L = 0.3\ \text{ps}$, $\lambda = 1\ \mu\text{m}$, $Q_e = 10\,\text{pc}$, and $W_\gamma = 10\ \text{mJ}$. Note that no nonlinear effects were included in this

ODU Compton Light Source

01 June 2015

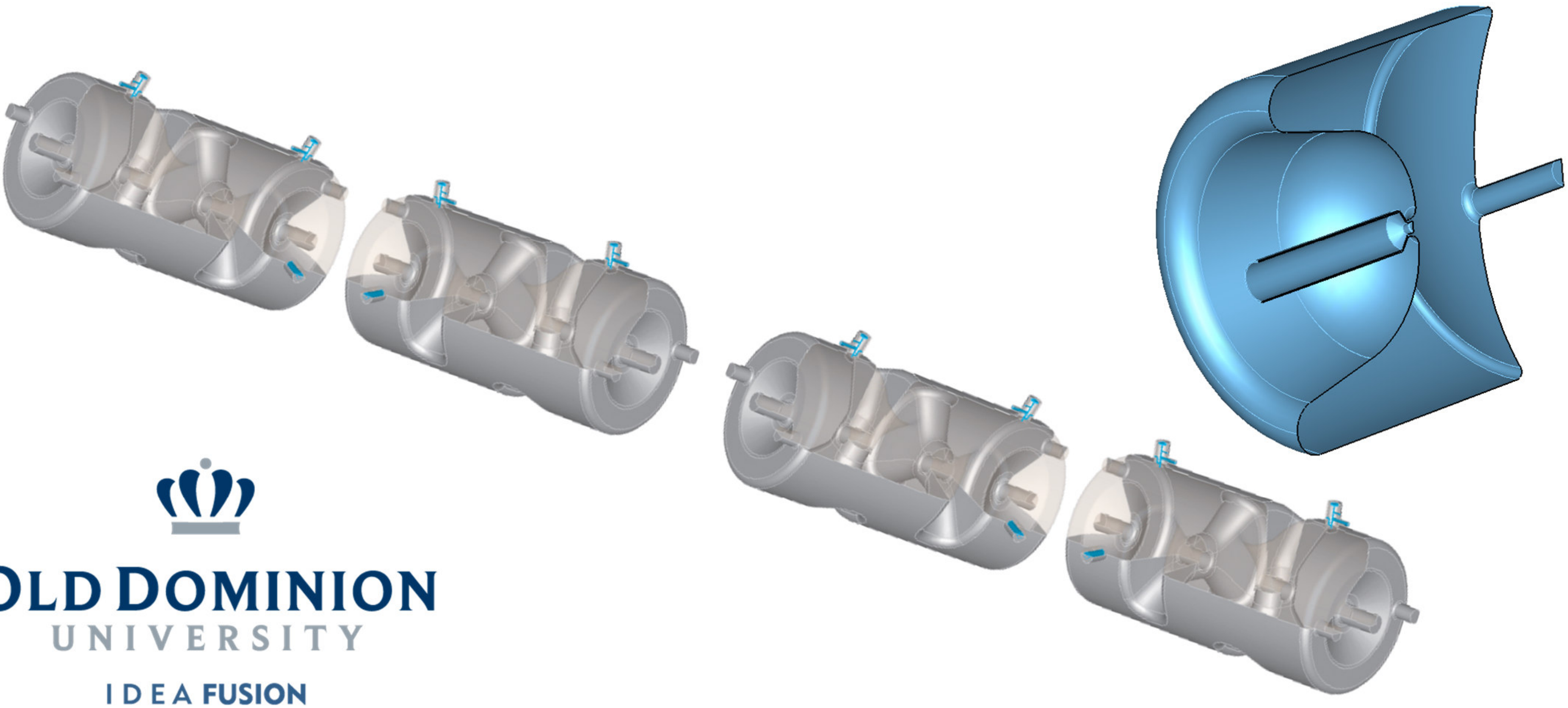

OLD DOMINION UNIVERSITY

IDEA FUSION

Parameters

Parameter	Quantity	Units
Energy	25	MeV
Bunch charge	10	pC
Repetition rate	100	MHz
Average current	1	mA
Trans. norm. emittance	0.1	mm-mrad
$\beta_{x,y}$	5	mm
FWHM bunch length	3.0 (0.9)	psec (mm)
RMS energy spread	7.5	keV

Electron beam parameters at collision point.

Parameters

Parameter	Quantity	Units
Wavelength	1 (1.24)	μm (eV)
Circulating power	1	MW
Number of photons/bunch	5×10^{16}	
Spot size	3.2	μm
Peak strength	0.026	
X-ray energy	Up to 12	keV
Photons/bunch	1.6×10^{6}	
Flux	1.6×10^{14}	photon/sec
Avg. brilliance	1.6×10^{15}	photon/(sec-mm^2-mrad^2-0.1%BW)

Optical cavity parameters.

Compton source parameters.

Electron gun

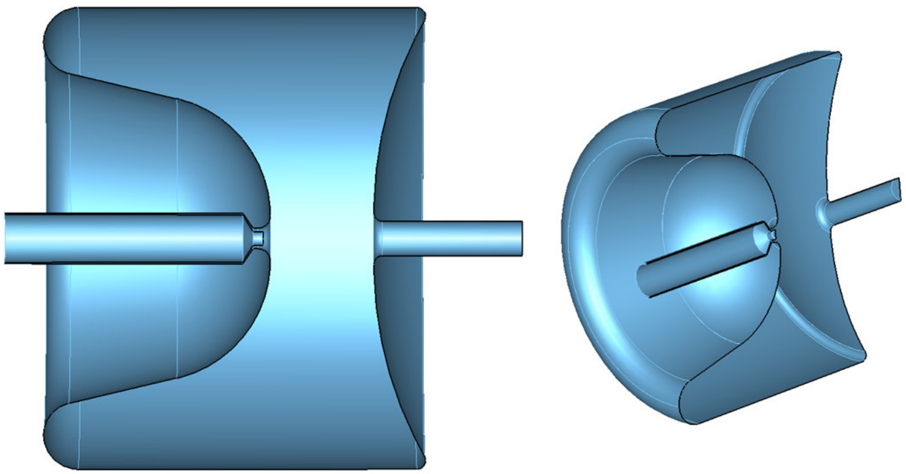

- Originally based on quarter-wave SRF electron gun developed by Harris *et al*.
- Highly reentrant to mitigate growth of normalized emittance due to space charge.

Parameter	Quantity	Units
Freq. of accele-rating mode	499.3	MHz
$\lambda/4$	150	mm
Design β	0.95	
Stored energy	44	mJ
QR_S	83.5	Ω
R/Q	154	Ω
Peak electric surface field (E_P)	3.67	MV/m
Peak magnetic surface field (B_P)	6.64	mT
E_P/B_P	1.81	mT/(MV/m)

RF Properties at E_{acc} = 1 MV/m

Electron gun

- EM fields calculated by SUPERFISH
- Particle tracking simulated by ASTRA
- Diameter/length 30 cm
- Beam travels 15 cm

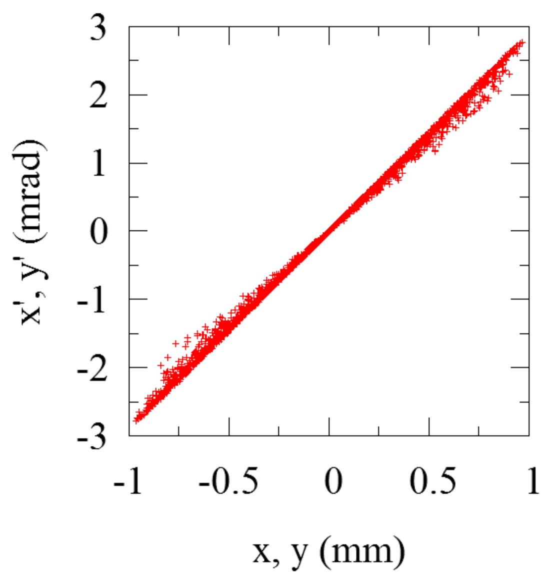

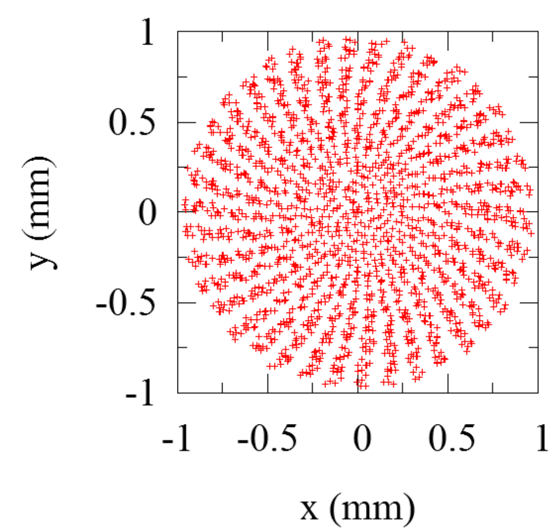

Top: Transverse phase space and spot.
Bottom: Electron beam properties at gun exit.

Parameter	Quantity	Units
E_{kin}	1.55	MeV
RMS Energy spread	0.526	keV
$\sigma_{x,y}$	0.477	mm
Normalized RMS $\varepsilon_{x,y}$	0.12	mm-mrad

Linac

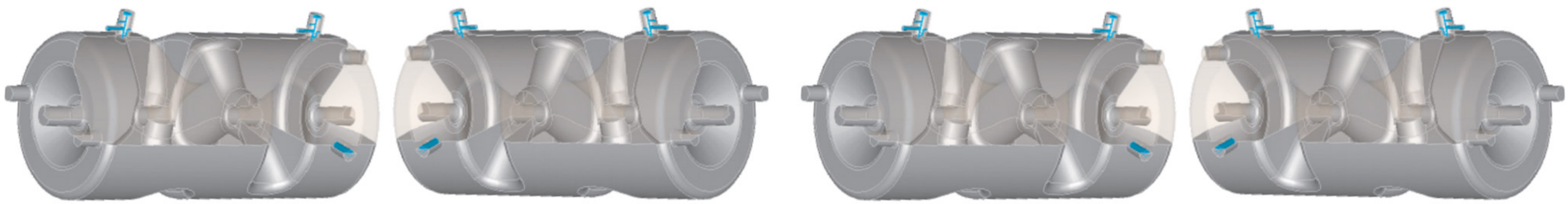

- Consists of 4 high-velocity, double-spoke cavities.
- Alternating orientation to produce roundest beam at exit.

- 500 MHz
- Diameter of 41.6 cm
- Length of 80.5 cm

- EM fields calculated by CST Microwave Studio.
- Particle tracking simulated by ASTRA.

- Entire accelerating section has 5 m x 1 m footprint

Linac

Parameter	Quantity	Units
Energy	25.02	MeV
RMS Energy spread	31.09	keV
σ_z	2.1 (7.0)	mm (psec)
$\sigma_{x,y}$	0.511, 0.482	mm
Norm. RMS $\varepsilon_{x,y}$	0.16, 0.15	mm-mrad
$\alpha_{x,y}$	2.34, -0.591	
$\beta_{x,y}$	82.7, 75.5	m

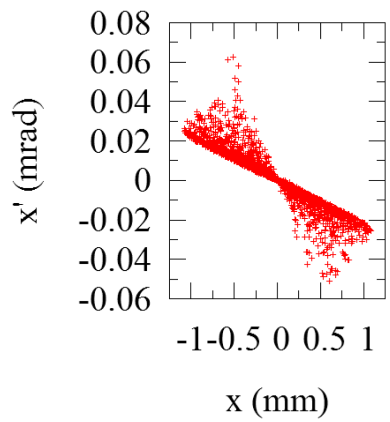

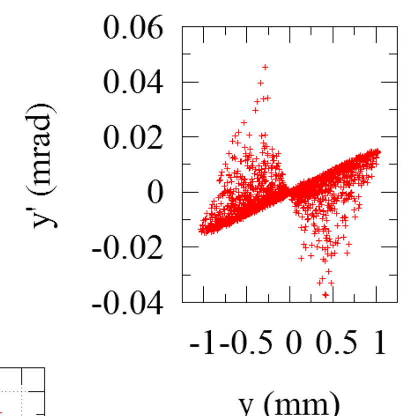

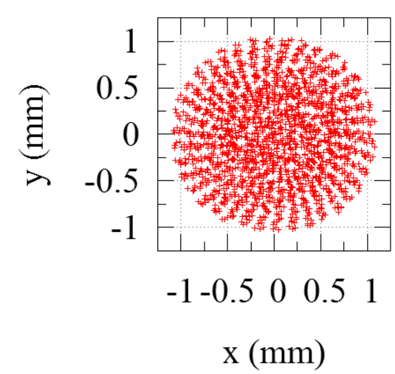

❖ Transverse phase spaces are bowties, not ellipses.

Top: Electron beam properties at linac exit.
Bottom: Transverse phase spaces and beam spot.

Matching

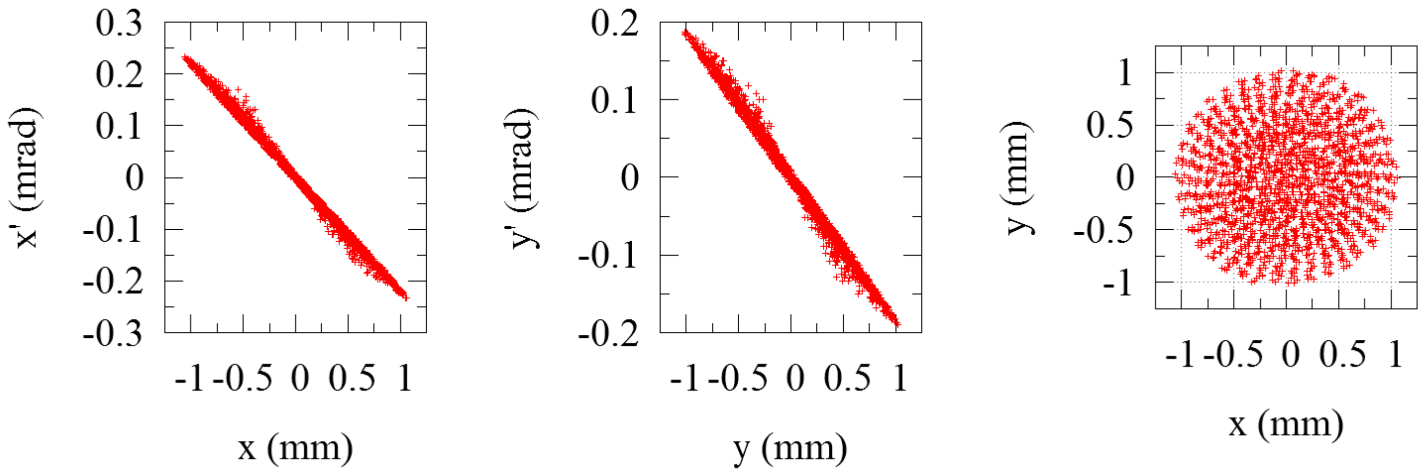

- Solenoid transforms bowties into phase spaces.
- Normalized RMS $\varepsilon_{x,y}$: 0.16, 0.15 → 0.19, 0.18 mm-mrad.
- As solenoid strength increases, so does emittance growth.
- Followed by a quadrupole and skew quadrupole, to get $\alpha_x = \alpha_y$ and to remove *x'y'* coupling, respectively.
- ~1 m in length.
- Modeled by elegant.

Bunch Compressor

- Consists of four dipole s-chicane.
- Two designs:
  - 3π phase advance (symmetric dispersion)
  - 4π phase advance (antisymmetric dispersion)
- M_{56} is tunable by adjusting bend angle of inner dipole pair.
- Sextupoles to remove longitudinal curvature.
- Followed by uncoupling and final focusing sections.
- Modeled by elegant.

Tunable M_{56}

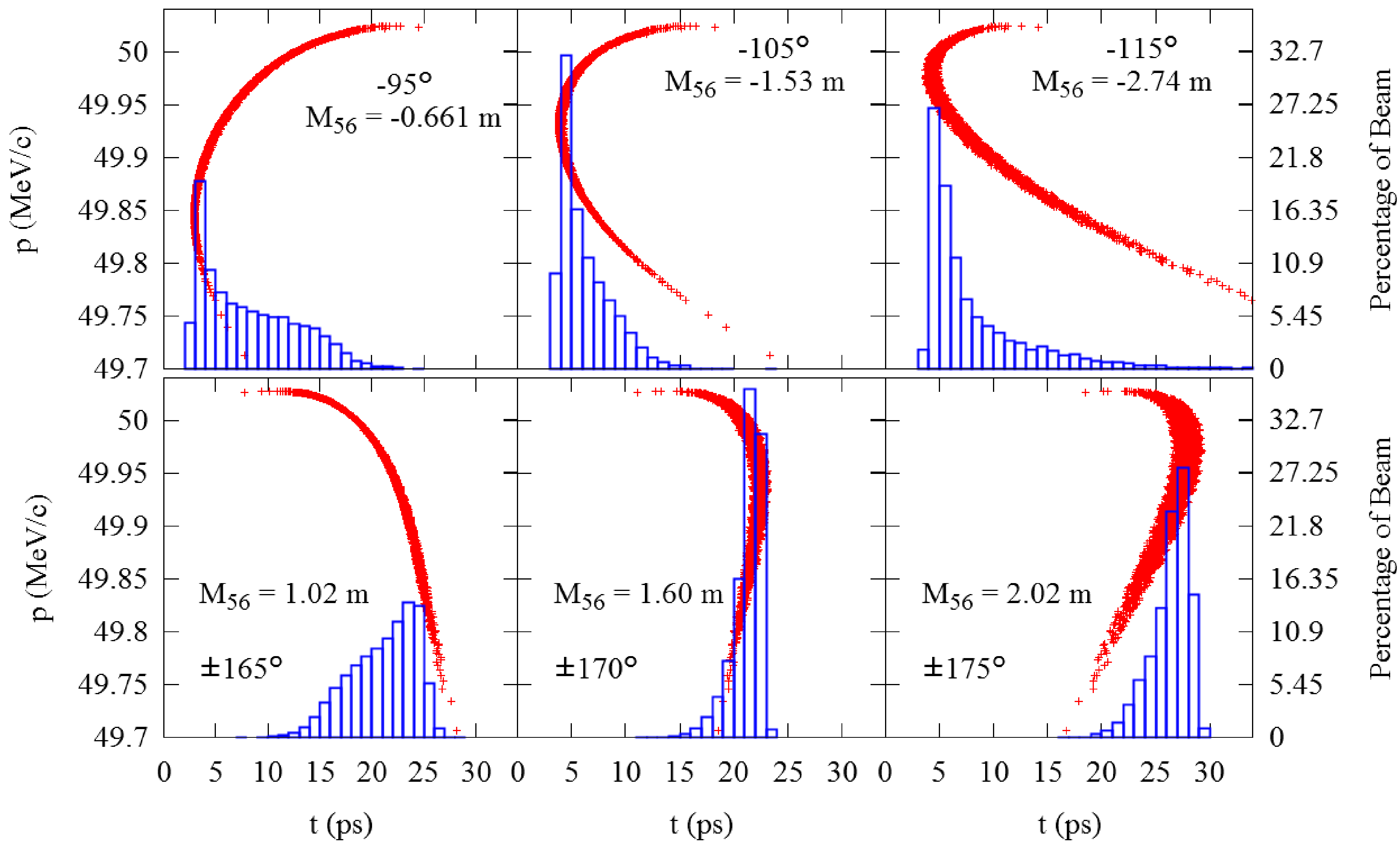

-95°
M56 = -0.661 m
-105°
M56 = -1.53 m
-115°
M56 = -2.74 m
M56 = 1.02 m
±165°
M56 = 1.60 m
±170°
M56 = 2.02 m
±175°
p (MeV/c)
Percentage of Beam
t (ps)
50
49.95
49.9
49.85
49.8
49.75
49.7
32.7
27.25
21.8
16.35
10.9
5.45
0
0 5 10 15 20 25 30

3π Design

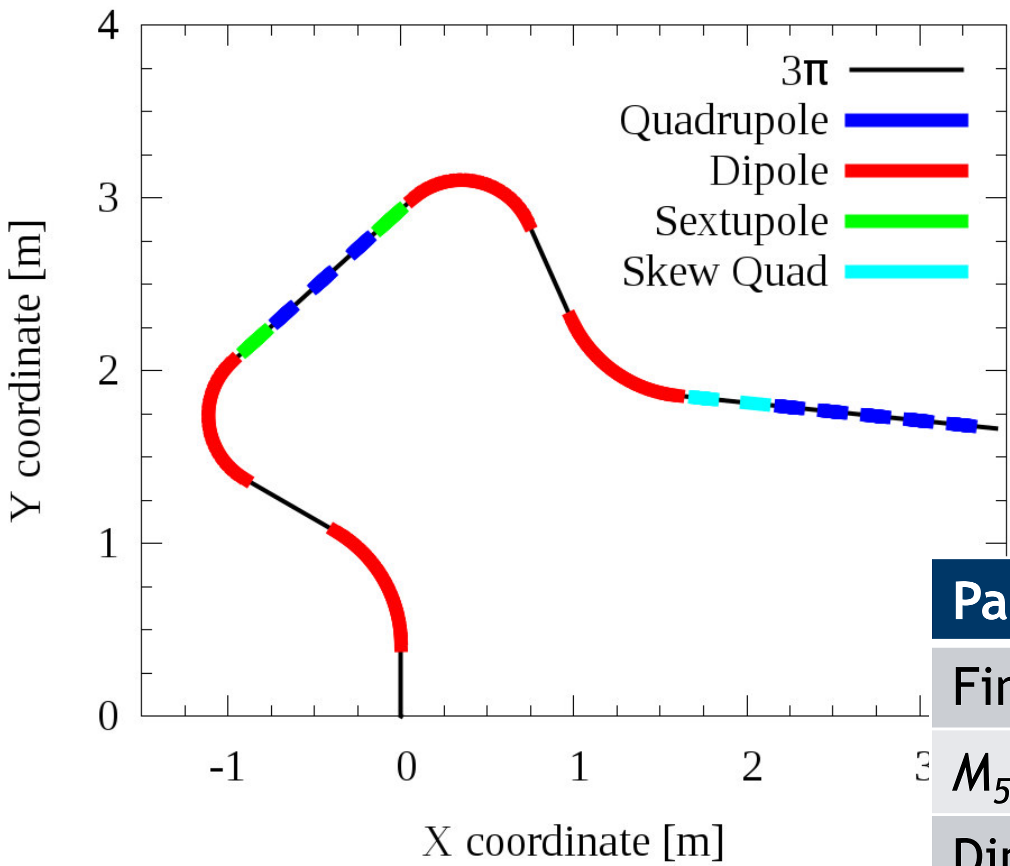

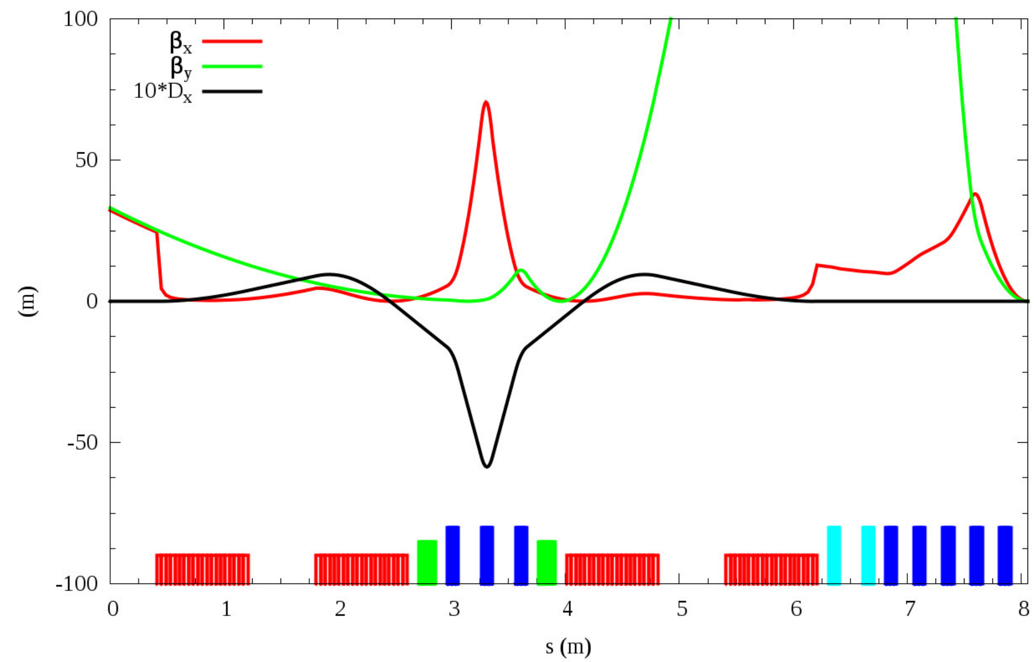

Parameter	Quantity	Units
Final $\beta_{x,y}$	5, 8	mm
M_{56}	-1.52	m
Dipole lengths	0.8, 0.8, 0.8, 0.8	m
Dipole bend angles	60, -108, -108, 60	°

4π Design

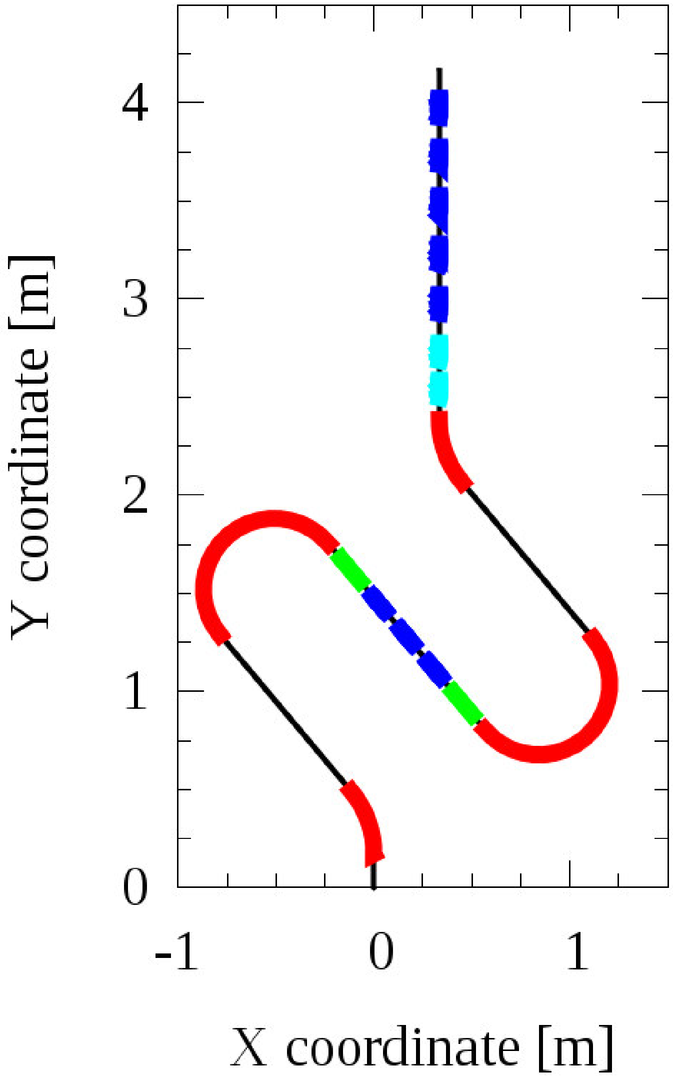

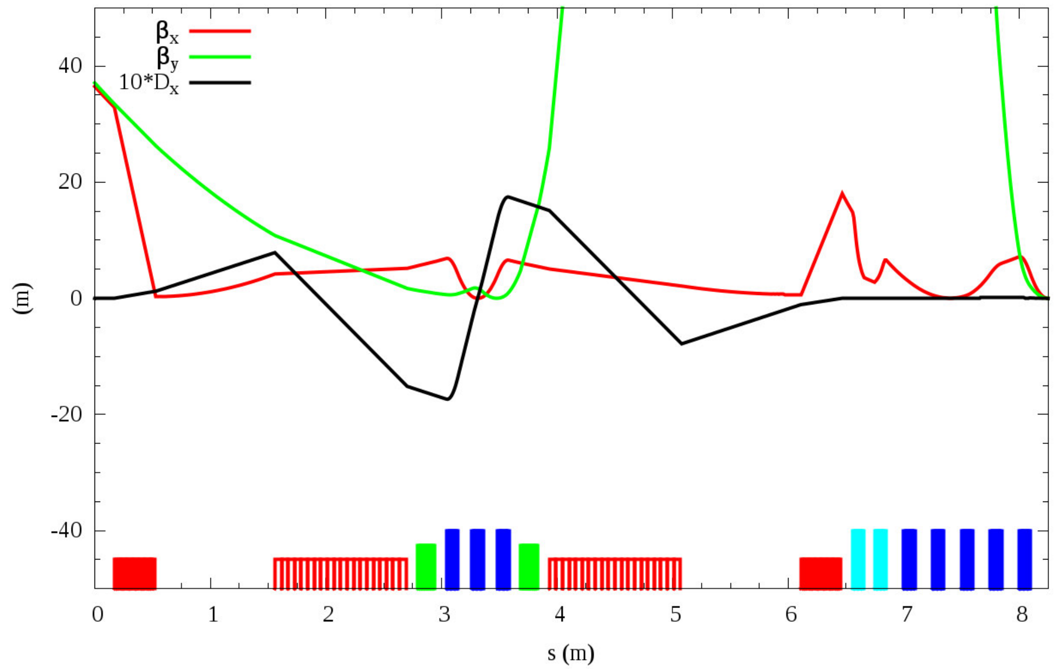

Parameter	Quantity	Units
Final $\beta_{x,y}$	6, 11	mm
M_{56}	1.39	m
Dipole lengths	0.35,1.1,1.1,0.35	m
Dipole bend angles	40,-180,180,-40	°

Beam spot and phase spaces

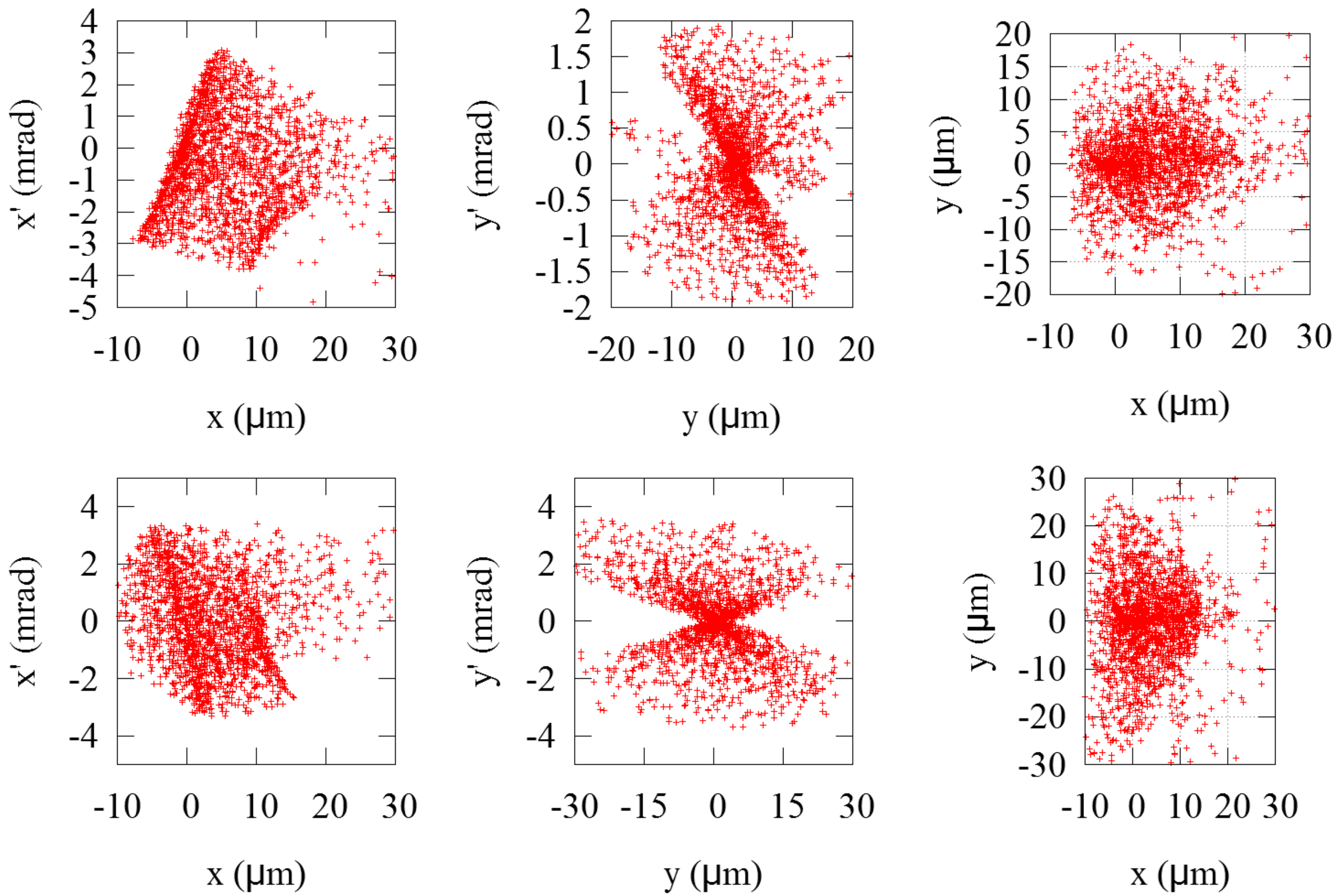

Results vs Goals

Parameter	Goal	3π Design	4π Design	Units
Energy	25	25.02		MeV
RMS energy spread	7.5	31.09		keV
FWHM bunch length	3.0 (0.9)	2	2	psec (mm)
Normalized RMS $\varepsilon_{x,y}$	0.1	0.6,0.3	0.6,1.4	mm-mrad
$\beta_{x,y}$	5	5, 8	6, 11	mm
$\sigma_{x,y}$	3.2	7, 8	9, 18	μm

Summary

- Compton sources of high energy photons have existed for about thirty years
- The have followed the usual progression: [1] borrow an existing machine (1st generation), and [2] make it better by technological innovation (2nd generation?)
- We are perhaps approaching 3rd generation devices, i.e., electron accelerators specifically designed for Compton/Thomson sources. ODU or Uppsala design?
- Our design ideas are having “convergence” with high energy collider design ideas
- Lots of ideas, but still looking for the “killer ap”.

Summary

- A “new” calculation scheme for high intensity pulsed laser Thomson Scattering has been developed. This same scheme can be applied to calculate spectral properties of “short”, high-*K* wigglers, and to compute optimal incident laser chirping.
- Due to ponderomotive broadening, it is simply wrong to use single-frequency estimates of flux in many situations
- The new theory is needed for Thomson scattering of Table Top TeraWatt lasers, which have exceedingly high field and short pulses. Proper laser chirping is important in this regime.